

Lattice Wess-Zumino model with Ginsparg-Wilson fermions: One-loop results and GPU benchmarks

Chen Chen,^{*} Eric Dzienkowski,[†] and Joel Giedt[‡]

*Department of Physics, Applied Physics and Astronomy,
Rensselaer Polytechnic Institute, 110 8th Street, Troy NY 12065 USA*

(Dated: November 6, 2018)

Abstract

We numerically evaluate the one-loop counterterms for the four-dimensional Wess-Zumino model formulated on the lattice using Ginsparg-Wilson fermions of the overlap (Neuberger) variety, together with an auxiliary fermion (plus superpartners), such that a lattice version of $U(1)_R$ symmetry is exactly preserved in the limit of vanishing bare mass. We confirm previous findings by other authors that at one loop there is no renormalization of the superpotential in the lattice theory, but that there is a mismatch in the wavefunction renormalization of the auxiliary field. We study the range of the Dirac operator that results when the auxiliary fermion is integrated out, and show that localization does occur, but that it is less pronounced than the exponential localization of the overlap operator. We also present preliminary simulation results for this model, and outline a strategy for nonperturbative improvement of the lattice supercurrent through measurements of supersymmetry Ward identities. Related to this, some benchmarks for our graphics processing unit code are provided. Our simulation results find a nearly vanishing vacuum expectation value for the auxiliary field, consistent with approximate supersymmetry at weak coupling.

PACS numbers: 11.15.Ha, 11.30.Pb

^{*}Electronic address: chenc10@rpi.edu

[†]Electronic address: dziene@rpi.edu

[‡]Electronic address: giedtj@rpi.edu

I. INTRODUCTION

One would like to have a general method for studying strongly coupled supersymmetric field theories with lattice techniques. This is because nonperturbative dynamics play an important role in the theory of supersymmetry breaking and its transmission to the visible sector of particle physics. In this article we examine one such general method, which involves a fine-tuning of bare lattice parameters, after having restricted the number of counterterms using lattice symmetries. At the same time, we perform detailed numerical studies of a lattice formulation that was studied by several groups a few years ago [1–6]. We will highlight some interesting features of that model and present some new results regarding locality of the lattice Dirac operator and the degree of explicit supersymmetry breaking that occurs.

Four-dimensional supersymmetric models on the lattice¹ generically require fine-tuning of counterterms. This is to be contrasted with lower dimensional theories where lattice symmetries can eliminate the need for such fine-tuning; see [10] for further details. The one known four-dimensional exception is pure $\mathcal{N} = 1$ super-Yang-Mills using Ginparg-Wilson fermions; the domain wall variety has been the subject of past [13] and recent [9, 14–18] simulations. Clearly we would like to go beyond pure $\mathcal{N} = 1$ super-Yang-Mills. Recently it was proposed [19] that an acceptable amount of fine-tuning could be efficiently performed using a multicanonical Monte Carlo [20] simulation together with Ferrenberg-Swendsen reweighting [21–23] in a large class of theories; see also [9]. In this approach it is necessary to design the multicanonical reweighting function. We had suggested beginning at weak coupling on small lattices, using the one-loop perturbative counterterms as initial conditions to an iterative search approach. The present article reports numerical results for one-loop calculations in lattice perturbation theory that are designed to locate this starting point. Ironically we find that for the lattice theory that is studied here, the one-loop counterterms are entirely wavefunction renormalization, and that the logarithmically divergent parts match for the scalar and fermion. As a result, the initial condition for the iterative search is equivalent to starting with the tree-level action, since it is just a rescaling of the fields. This lends interest to our simulation results for the action with no fine-tuning, which we report here.

The theory that we study is the four-dimensional Wess-Zumino model, formulated on the lattice with a variant of overlap (Neuberger) fermions [24]. The goal of the formulation is to impose the Majorana condition and simultaneously preserve the chiral $U(1)_R$ symmetry [1–6] that is present in the continuum in the massless limit. As will be seen, preserving this symmetry greatly limits the number of counterterms that must be fine-tuned in order to obtain the supersymmetric continuum limit. In addition to overlap fermions, the lattice formulation has auxiliary fermions (plus superpartner fields) that couple to the overlap fermions through the Yukawa coupling, as in [25]. It is possible to integrate out the auxiliary

¹ For reviews with extensive references see [7–12].

fermions (and superpartner fields), and when one does this a nonanalytic Dirac operator results for the surviving fermionic field. Thus, as has been discussed originally in [1], and at greater length in [2, 5] the action is singular once auxiliary fields are integrated out. However, as we describe below, there is a sensible resolution of this singularity by taking the theory to “live” inside a finite box, with antiperiodic boundary conditions in the time direction for the fermions. The singularity of the Dirac operator that this resolves is related to nonpropagating modes in the infinite volume limit; the fact that these are nonpropagating was shown in [6]. However, singularities in the Dirac operator raise the spectre of possible nonlocalities in the continuum limit, as was found in gauge theories with the SLAC derivative [26]. By analogy to that study, we have analyzed the continuum limit of the scalar self-energy and find that it is analytic in p^2 , so that there is no sign of nonlocality. We have also measured the degree of localization of the Dirac operator following the approach of [27]. We find that while there is localization, it is less pronounced than the exponential localization of the overlap operator. In the process of discussing our numerical perturbative results we are able to highlight the divergence structure of this theory, which turns out to be strictly wave function renormalization at one-loop. The wave function renormalization of the fermion and the physical scalar match at one loop in the continuum limit of the lattice expressions; but, the auxiliary scalar has a mismatched wave function counterterm. These findings appeared previously in [1]; thus we confirm those results.

Having discussed the perturbative results, we then review correlation functions and renormalization constants that must be measured in the simulations in order to fine-tune the theory. These involve the renormalized supercurrent (the current is renormalized because the symmetry is broken by the lattice regulator). We conclude with preliminary simulation results. In particular, we have developed all of the components for simulations on graphics processing units. Benchmarks that characterize the performance of our code are reported here. We measure one broken Ward-Takahashi identity in a simulation and find it to be very small at weak coupling. We argue that this is consistent with the nonrenormalization of the superpotential at one loop in lattice perturbation theory.

II. DEFINITIONS

A. Continuum

The Euclidean continuum theory has action

$$\begin{aligned}
 S &= - \int d^4x \left\{ \frac{1}{2} \chi^T C M \chi + \phi^* \square \phi + F^* F + F^* (m^* \phi^* + g^* \phi^{*2}) + F (m \phi + g \phi^2) \right\}, \\
 M &= \not{\partial} + (m + 2g\phi) P_+ + (m^* + 2g^* \phi^*) P_-.
 \end{aligned} \tag{2.1}$$

Our conventions will be ($i = 1, 2, 3$):

$$\begin{aligned} \gamma_0 &= \begin{pmatrix} 0 & 1 \\ 1 & 0 \end{pmatrix}, & \gamma_i &= \begin{pmatrix} 0 & i\sigma_i \\ -i\sigma_i & 0 \end{pmatrix}, & \gamma_5 &= \begin{pmatrix} -1 & 0 \\ 0 & 1 \end{pmatrix}, \\ P_{\pm} &= \frac{1}{2}(1 \pm \gamma_5), & C &= \gamma_0\gamma_2. \end{aligned} \quad (2.2)$$

It can be checked that the action is invariant under the supersymmetry transformations

$$\begin{aligned} \delta_\epsilon\phi &= \sqrt{2}\epsilon^T CP_+\chi, & \delta_\epsilon\phi^* &= \sqrt{2}\epsilon^T CP_-\chi, \\ \delta_\epsilon\chi &= -\sqrt{2}P_+(\not{\partial}\phi + F)\epsilon - \sqrt{2}P_-(\not{\partial}\phi^* + F^*)\epsilon, \\ \delta_\epsilon F &= \sqrt{2}\epsilon^T C\not{\partial}P_+\chi, & \delta_\epsilon F^* &= \sqrt{2}\epsilon^T C\not{\partial}P_-\chi \end{aligned} \quad (2.3)$$

Note also that in momentum space

$$-\phi^*\square\phi \rightarrow |\phi(p)|^2 p^2 \quad (2.4)$$

so that for a well defined partition function we must take the negative sign in the exponent:

$$Z = \int [d\phi \, d\phi^* \, dF \, dF^* \, d\chi] e^{-S} \quad (2.5)$$

On the other hand, integration over the auxiliary field F is not well-defined (as is usual in Euclidean formulations of supersymmetric theories). In particular, we have after integrating out the fermions and completing the square,

$$\begin{aligned} Z &= \int [d\phi \, d\phi^*] e^{-S(\phi)} \text{Pf}CM(\phi) \int [dF \, dF^*] \exp \int d^4x |F^* + m\phi + g\phi^2|^2, \\ S(\phi) &= \int d^4x (-\phi^*\square\phi + |m\phi + g\phi^2|^2) \end{aligned} \quad (2.6)$$

where $\text{Pf}CM$ is the Pfaffian of the matrix CM . Under shift of integration variables

$$F \rightarrow F' = F + m^*\phi^* + g^*\phi^{*2}, \quad F^* \rightarrow F'^* = F^* + m\phi + g\phi^2 \quad (2.7)$$

Z does not converge, due to the auxiliary field factor $\int [dF' \, dF'^*] \exp \int d^4x |F'|^2$. This fact was noted, for example, in [1] where they simply divide by an infinite constant—the partition function of the $g = 0$ theory—to cancel the infinity. In a lattice simulation we do not have this luxury, and we must decide on the proper way to deal with the integration over F, F^* .

Of course in the Minkowski space formulation, due to the presence of an additional factor $-i$, the integral over the auxiliary fields F', F'^* can be computed by analytic continuation. One discards the overall constant into the normalization of Z , and the net result is that one imposes the equations of motion:

$$\frac{\delta S}{\delta F(x)} = \frac{\delta S}{\delta F^*(x)} = 0. \quad (2.8)$$

From this we conclude that in Euclidean space the integral (2.6) should be understood in a formal sense; it is an instruction to impose (2.8). This is equivalent to completing the square, as in (2.6), shifting the integration variable and then ignoring the (infinite) constant factor that is generated. Thus all simulations are performed with the action in the form with the auxiliary fields removed. In this form the supersymmetry transformations are nonlinear and the supersymmetry algebra only closes on-shell.

B. Lattice

We next discuss the lattice action, which is a special case of the formulations of [1, 2]; we write the lattice action in forms given in [4–6]. For this, a few lattice derivative operators must be introduced.

$$\begin{aligned}
A &= 1 - aD_W, \quad D_W = \frac{1}{2}\gamma_\mu(\partial_\mu^* + \partial_\mu) + \frac{1}{2}a\partial_\mu^*\partial_\mu \\
D_1 &= \frac{1}{2}\gamma_\mu(\partial_\mu^* + \partial_\mu)(A^\dagger A)^{-1/2} \\
D_2 &= \frac{1}{a} \left[1 - \left(1 + \frac{1}{2}a^2\partial_\mu^*\partial_\mu \right) (A^\dagger A)^{-1/2} \right] \\
D &= D_1 + D_2 = \frac{1}{a} (1 - A(A^\dagger A)^{-1/2})
\end{aligned} \tag{2.9}$$

where ∂_μ and ∂_μ^* are the forward and backward difference operators respectively. Then the lattice action is [5]:

$$\begin{aligned}
S &= -a^4 \sum_x \left\{ \frac{1}{2}\chi^T C D \chi + \phi^* D_1^2 \phi + F^* F + F D_2 \phi + F^* D_2 \phi^* \right. \\
&\quad - \frac{1}{a} X^T C X - \frac{2}{a} (\mathcal{F} \Phi + \mathcal{F}^* \Phi^*) \\
&\quad + \frac{1}{2} \tilde{\chi}^T C \left(m P_+ + m^* P_- + 2g \tilde{\phi} P_+ + 2g^* \tilde{\phi}^* P_- \right) \tilde{\chi} \\
&\quad \left. + \tilde{F}^* (m^* \tilde{\phi}^* + g^* \tilde{\phi}^{*2}) + \tilde{F} (m \tilde{\phi} + g \tilde{\phi}^2) \right\}
\end{aligned} \tag{2.10}$$

Here, the tilded fields are the linear combinations

$$\tilde{\phi} = \phi + \Phi, \quad \tilde{\chi} = \chi + X, \quad \tilde{F} = F + \mathcal{F} \tag{2.11}$$

The fields Φ, X, \mathcal{F} and their conjugates are auxiliary fields introduced to allow for a lattice realization of the chiral $U(1)_R$ symmetry in the $m \rightarrow 0$ limit:

$$\begin{aligned}
\delta\chi &= i\alpha\gamma_5 \left(1 - \frac{a}{2}D\right) \chi + i\alpha\gamma_5 X, & \delta X &= i\alpha\gamma_5 \frac{a}{2}D\chi, \\
\delta\phi &= -3i\alpha\phi + i\alpha \left[\left(1 - \frac{a}{2}D_2\right) \phi - \frac{a}{2}F^* \right] + i\alpha\Phi, \\
\delta\Phi &= -3i\alpha\Phi + i\frac{a}{2}\alpha (D_2\phi + F^*) \\
\delta F &= 3i\alpha F + i\alpha \left[\left(1 - \frac{a}{2}D_2\right) F - \frac{a}{2}D_1^2\phi^* \right] + i\alpha\mathcal{F} \\
\delta\mathcal{F} &= 3i\alpha\mathcal{F} + i\frac{a}{2}\alpha (D_2F + D_1^2\phi^*)
\end{aligned} \tag{2.12}$$

which takes a particularly simple form on the tilded variables:

$$\delta\tilde{\chi} = i\alpha\gamma_5\tilde{\chi}, \quad \delta\tilde{\phi} = -2i\alpha\tilde{\phi}, \quad \delta\tilde{F} = 4i\alpha\tilde{F} \tag{2.13}$$

The supersymmetry transformations of the untilded fields will be taken as

$$\begin{aligned}
\delta_\epsilon\phi &= \sqrt{2}\epsilon^T CP_+\chi, & \delta_\epsilon\phi^* &= \sqrt{2}\epsilon^T CP_-\chi, \\
\delta_\epsilon\chi_\beta &= -\sqrt{2}(P_+(D_1\phi + F)\epsilon)_\beta - \sqrt{2}(P_-(D_1\phi^* + F^*)\epsilon)_\beta, \\
\delta_\epsilon F &= \sqrt{2}\epsilon^T CD_1P_+\chi, & \delta_\epsilon F^* &= \sqrt{2}\epsilon^T CD_1P_-\chi
\end{aligned} \tag{2.14}$$

and for the auxiliary multiplet

$$\begin{aligned}
\delta_\epsilon\Phi &= \sqrt{2}\epsilon^T CP_+X, & \delta_\epsilon\Phi^* &= \sqrt{2}\epsilon^T CP_-X, \\
\delta_\epsilon X_\beta &= -\sqrt{2}(P_+(D_1\Phi + \mathcal{F})\epsilon)_\beta - \sqrt{2}(P_-(D_1\Phi^* + \mathcal{F}^*)\epsilon)_\beta, \\
\delta_\epsilon\mathcal{F} &= \sqrt{2}\epsilon^T CD_1P_+X, & \delta_\epsilon\mathcal{F}^* &= \sqrt{2}\epsilon^T CD_1P_-X
\end{aligned} \tag{2.15}$$

Of course this is not a symmetry of the lattice action for $g \neq 0$. Here we are just choosing the form of the transformation that will be used to generate broken Ward-Takahashi identities on the lattice. The supersymmetry transformations of the tilded fields are

$$\begin{aligned}
\delta_\epsilon\tilde{\phi} &= \sqrt{2}\epsilon^T CP_+\tilde{\chi}, & \delta_\epsilon\tilde{\phi}^* &= \sqrt{2}\epsilon^T CP_-\tilde{\chi}, \\
\delta_\epsilon\tilde{\chi}_\beta &= -\sqrt{2}(P_+(D_1\tilde{\phi} + \tilde{F})\epsilon)_\beta - \sqrt{2}(P_-(D_1\tilde{\phi}^* + \tilde{F}^*)\epsilon)_\beta, \\
\delta_\epsilon\tilde{F} &= \sqrt{2}\epsilon^T CD_1P_+\tilde{\chi}, & \delta_\epsilon\tilde{F}^* &= \sqrt{2}\epsilon^T CD_1P_-\tilde{\chi}
\end{aligned} \tag{2.16}$$

As noted in [5], we can integrate out the auxiliary fields X, Φ, \mathcal{F} , treating the tilded fields as constant, to obtain the lattice action:²

$$\begin{aligned}
S &= -a^4 \sum_x \left\{ \frac{1}{2}\tilde{\chi}^T CM\tilde{\chi} - \frac{2}{a}\tilde{\phi}^* D_2\tilde{\phi} + \tilde{F}^*(1 - \frac{a}{2}D_2)^{-1}\tilde{F} \right. \\
&\quad \left. + \tilde{F}^*(m^*\tilde{\phi}^* + g^*\tilde{\phi}^{*2}) + \tilde{F}(m\tilde{\phi} + g\tilde{\phi}^2) \right\}.
\end{aligned} \tag{2.17}$$

² Integrating out an auxiliary fermion to obtain the fermionic part of this action was previously noted in [2]. There it was noted that this relates the fermionic action to the one of [25] by a singular field transformation. This singularity will be discussed more in Section III below.

This is the lattice action Eq. (2.14) of [4] with a notation that interchanges $D_1 \leftrightarrow D_2$, which is equivalent to Eq. (2.22) of [2] for the $k = 0$ case, using the identities³

$$\Gamma_5 = \gamma_5(1 - \frac{a}{2}D), \quad \Gamma_5^2 = 1 - \frac{a}{2}D_2, \quad D^\dagger D = \frac{2}{a}D_2. \quad (2.18)$$

The fermion matrix is:

$$M = \mathcal{D} + mP_+ + m^*P_- + 2g\tilde{\phi}P_+ + 2g^*\tilde{\phi}^*P_-, \quad \mathcal{D} = (1 - \frac{a}{2}D_2)^{-1}D_1 \quad (2.19)$$

This way of writing the Dirac operator can be related to the one that appears in [2] by the identity:

$$(1 - \frac{a}{2}D_2)^{-1}D_1 = (1 - \frac{a}{2}D)^{-1}D \quad (2.20)$$

Furthermore we can integrate out the auxiliary fields \tilde{F}, \tilde{F}^* to obtain the action

$$S = a^4 \sum_x \left\{ -\frac{1}{2}\tilde{\chi}^T C M \tilde{\chi} + \frac{2}{a}\tilde{\phi}^* D_2 \tilde{\phi} + (m^*\tilde{\phi}^* + g^*\tilde{\phi}^{*2})(1 - \frac{a}{2}D_2)(m\tilde{\phi} + g\tilde{\phi}^2) \right\} \quad (2.21)$$

This is the action that is used in our numerical simulations.

When fine-tuning of the lattice action is performed, we must invoke the most general lattice action consistent with symmetries. Since we perform our simulations at $m \neq 0$, this is just the action with all dimension ≤ 4 operators built out of the physical fields, $\tilde{\phi}$ and $\tilde{\chi}$. We write it here for reference:

$$\begin{aligned} S = a^4 \sum_x \left\{ -\frac{1}{2}\tilde{\chi}^T C (\mathcal{D} + m_1P_+ + m_1^*P_-)\tilde{\chi} + \frac{2}{a}\tilde{\phi}^* D_2 \tilde{\phi} \right. \\ \left. + m_2^2|\tilde{\phi}|^2 + \lambda_1|\tilde{\phi}|^4 + (m_3^2\tilde{\phi}^2 + g_1\tilde{\phi}^3 + g_2\tilde{\phi}\tilde{\phi}^{*2} + \lambda_2\tilde{\phi}^4 + \lambda_3\tilde{\phi}\tilde{\phi}^{*3} + \text{h.c.}) \right. \\ \left. - \tilde{\chi}^T C (y_1\tilde{\phi}P_+ + y_1^*\tilde{\phi}^*P_-)\tilde{\chi} - \tilde{\chi}^T C (y_2\tilde{\phi}P_- + y_2^*\tilde{\phi}^*P_+)\tilde{\chi} \right\} \quad (2.22) \end{aligned}$$

A term linear in $\tilde{\phi}$ has been eliminated by the redefinition $\tilde{\phi} \rightarrow \tilde{\phi} + c$ with c a constant. The parameters m_2^2 and λ_1 are real and all other parameters are complex. Whereas in the supersymmetric theory there are four real parameters, in the most general theory we have eighteen real parameters to adjust. Holding m_1 and y_1 fixed, we have fourteen real parameters that must be adjusted to obtain the supersymmetric limit. The counting can be alleviated somewhat by imposing CP invariance, so that all parameters can be assumed real. Then we have a total of ten parameters. Holding two fixed, we must tune the other eight to achieve the supersymmetric limit. Conducting a fine-tuning in an eight-dimensional parameter space is a daunting task.

³ We thank A. Feo for explaining this point and providing us with a derivation of these relations.

On the other hand in the limit $m_1 \rightarrow 0$ we can impose the $U(1)_R$ symmetry (2.13). This restricts the action to

$$S = a^4 \sum_x \left\{ -\frac{1}{2} \tilde{\chi}^T C \mathcal{D} \tilde{\chi} + \frac{2}{a} \tilde{\phi}^* D_2 \tilde{\phi} + m_2^2 |\tilde{\phi}|^2 + \lambda_1 |\tilde{\phi}|^4 - \tilde{\chi}^T C (y_1 \tilde{\phi} P_+ + y_1^* \tilde{\phi}^* P_-) \tilde{\chi} \right\} \quad (2.23)$$

If we hold y_1 fixed, then only m_2^2 and λ_1 must be fine-tuned. Conducting a search in a two-dimensional parameter space, with both coming from bosonic terms, is manageable. The difficult part is that we must extrapolate to the massless fermion limit. Another potential problem is that we impose antiperiodic boundary conditions for the fermion in the time direction, but must impose periodic boundary conditions for the scalar in order for the action to be single-valued on the circle in the time direction. This breaks supersymmetry explicitly by boundary conditions. At finite mass this should be an effect that can be made arbitrarily small by taking the large volume limit. However at vanishing mass, there will be long distance modes that will “feel” the breaking due to boundary conditions.⁴ Thus it is important that we take $T \gg 1/ma$ as m is sent to zero, where T is the number of sites in the time direction.

As we will see, the one-loop behavior of the theory (2.17) closely follows that of the continuum, so that no new operators are generated at this order. Thus at this level of approximation, a fine-tuning of the general lattice action (2.22) is not needed. For reasons that will be clearer once we have presented our perturbative results, it is of interest to study the original lattice action (2.21) in our simulations, without any fine-tuning. By measuring the degree of supersymmetry breaking through supersymmetry Ward identities that are conserved in the continuum, we gain information about the higher orders and nonperturbative aspects of the lattice theory.

III. MODES, FEYNMAN RULES AND TILDE/UNTILDE EQUIVALENCE

A. Mode analysis

As to the the nonlocal operator $(1 - \frac{1}{2}aD_2)^{-1}$ that appears in the action (2.17), note that for smooth field configurations $aD_2 \sim a^2\Box$. Nevertheless, one may rightly worry about the effect of modes for which $D_2 \sim 1/a$. The spectrum of $1 - \frac{1}{2}aD_2$ can easily be calculated in momentum space:

$$(1 - \frac{1}{2}aD_2)(p) = \frac{1}{2} + \frac{1}{2} \frac{1 - 2 \sum_{\mu} \sin^2(p_{\mu}a/2)}{\sqrt{[1 - 2 \sum_{\mu} \sin^2(p_{\mu}a/2)]^2 + \sum_{\mu} \sin^2(p_{\mu}a)}} \quad (3.1)$$

⁴ We thank G. Bergner for raising this point.

One sees that there are zeros at $p_\mu a$ equal to all of the would-be doublers:

$$(\underline{\pi}, 0, 0, 0), \quad (\underline{\pi}, \underline{\pi}, 0, 0), \quad (\underline{\pi}, \underline{\pi}, \underline{\pi}, 0), \quad (\pi, \pi, \pi, \pi), \quad (3.2)$$

where the underline indicates all possible permutations. Thus the auxiliary field kinetic term appearing in (2.17) is singular, as was discussed in [1], and more at length in [2, 5, 6]. For the fermions we must also consider

$$D_1(p) = \frac{-ia^{-1} \sum_\mu \gamma_\mu \sin(p_\mu a)}{\sqrt{[1 - 2 \sum_\mu \sin^2(p_\mu a/2)]^2 + \sum_\mu \sin^2(p_\mu a)}} \quad (3.3)$$

Thus $D_1(p) = 0$ for the would-be doublers (3.2) and the fermion operator $(1 - \frac{1}{2}aD_2)^{-1}D_1$ is indeterminate. In [6] it was shown that in a limiting process of approaching these points in momentum space, $(1 - \frac{1}{2}aD_2)^{-1}D_1$ is divergent. Thus the would-be doublers are actually nonpropagating. Note that

$$(1 - \frac{1}{2}aD_2)^{-1}D_1\gamma_5 + \gamma_5(1 - \frac{1}{2}aD_2)^{-1}D_1 = 0 \quad (3.4)$$

which is how the lattice formulation manages to preserve $U(1)_R$ symmetry. This is not in conflict with the Nielsen-Ninomiya theorem [28, 29] precisely because the operator $(1 - \frac{1}{2}aD_2)^{-1}D_1$ is unbounded and therefore nonanalytic. One should then worry about locality since a nonanalytic Dirac operator might violate this property, as was true of the SLAC Dirac operator [26]. We will investigate this below. We will find numerically that it does show localization, though not as pronounced as the exponential localization of the overlap operator. In fact it has a long tail that is a cause of some concern. However our perturbative results in a later section show no sign of nonanalytic sickness in the scalar self-energy as a function of p^2 , which would be the analogue of the results of [26].

For the fermion, in our simulations, we address the difficulty of the indeterminate operator by taking the fermion field to be antiperiodic in the time direction and restrict considerations to finite lattices $L^3 \times T$ with T even. Taking T even is necessary in order to avoid other zeros of $(1 - \frac{1}{2}aD_2)$. This resolves the indeterminacies for all finite L, T with T even. One then defines the infinite spacetime volume theory rigorously as the limiting value $L, T \rightarrow \infty$. Unfortunately, the maximum eigenvalue of the fermion operator $(1 - \frac{1}{2}aD_2)^{-1}D_1$ diverges as $T \rightarrow \infty$, so that the fermion matrix becomes poorly conditioned at very large system size. For the $T = 32$ and $T = 64$ lattices that we study this does not prove to be a serious problem.

For the auxiliary field \tilde{F} , in our simulations, we formally integrate it out, leading to the action (2.21). For the modes with $(1 - \frac{a}{2}D_2)(p) = 0$ the scalar potential vanishes. However, the kinetic term $\frac{2}{a}\tilde{\phi}^*D_2\tilde{\phi}$ is nonvanishing on this modes, with $\frac{2}{a}D_2(p) = 4/a^2$. These modes are therefore suppressed in the path integral and are part of the cutoff theory.

In perturbation theory, one can arrange for the modes at $p_\mu a$ of the would-be doublers (3.2) to be nonpropagating, as ought to be based on the results of [6]. This nonpropagating

feature is incorporated into the Feynman diagram rules of [5], as we now explain. First we note that

$$\begin{aligned} & \left[-D_1 + \left(1 - \frac{a}{2}D_2\right) (m^*P_+ + mP_-) \right] \left[\left(1 - \frac{a}{2}D_2\right)^{-1} D_1 + (mP_+ + m^*P_-) \right] \\ &= \frac{2}{a}D_2 + |m|^2 \left(1 - \frac{a}{2}D_2\right). \end{aligned} \quad (3.5)$$

using the Ginsparg-Wilson relation, which in terms of D_1 and D_2 takes the form [4]

$$D_1^2 - D_2^2 = -\frac{2}{a}D_2 \quad (3.6)$$

Then we find that the fermion propagator can be written

$$\langle \tilde{\chi}(x) \tilde{\chi}^T(y) \rangle_C = a^{-4} \left(\frac{-D_1 + \left(1 - \frac{a}{2}D_2\right) (m^*P_+ + mP_-)}{\frac{2}{a}D_2 + |m|^2 \left(1 - \frac{a}{2}D_2\right)} \right) (x, y) \quad (3.7)$$

This propagator vanishes for the would-be doublers (3.2). It avoids the alternative form that comes from a straightforward inversion of the free Dirac operator $M_0 = \left(1 - \frac{a}{2}D_2\right)^{-1} D_1 + mP_+ + m^*P_-$:

$$\langle \tilde{\chi}(x) \tilde{\chi}^T(y) \rangle_C = -a^{-4} \left(\frac{\left(1 - \frac{a}{2}D_2\right)^{-1} D_1 - (m^*P_+ + mP_-)}{\frac{2}{a}D_2 \left(1 - \frac{a}{2}D_2\right)^{-1} + |m|^2} \right) (x, y) \quad (3.8)$$

which is indeterminate for the would-be doublers. In our perturbative analysis of Section IV below, we use the propagator (3.7). This allows us to use periodic boundary conditions for the one-loop calculations.

B. Locality

Following the numerical approach of [27] we can investigate the locality of the operator $\mathcal{D} = \left(1 - \frac{a}{2}D_2\right)^{-1} D_1$. In what follows, we impose the antiperiodic in time boundary conditions on the fermions. We introduce a unit point source η at the origin $x = 0$ and then compute

$$\psi(x) = \left[\left(1 - \frac{a}{2}D_2\right)^{-1} D_1 \eta \right] (x) \quad (3.9)$$

The ‘‘taxi-driver distance’’

$$r = \|x\|_1 = \sum_{\mu} (|x_{\mu}| \text{ or } |L_{\mu} - x_{\mu}|) \quad (3.10)$$

to the origin is defined; the shortest length is selected in each ‘‘or’’ statement, where L_{μ}/a is the number of lattice sites in the μ direction. One then computes the norm $\|\psi(x)\|$ in spinor index space at site x and obtains the function

$$f(r) = \max\{\|\psi(x)\| \mid \|x\|_1 = r\} \quad (3.11)$$

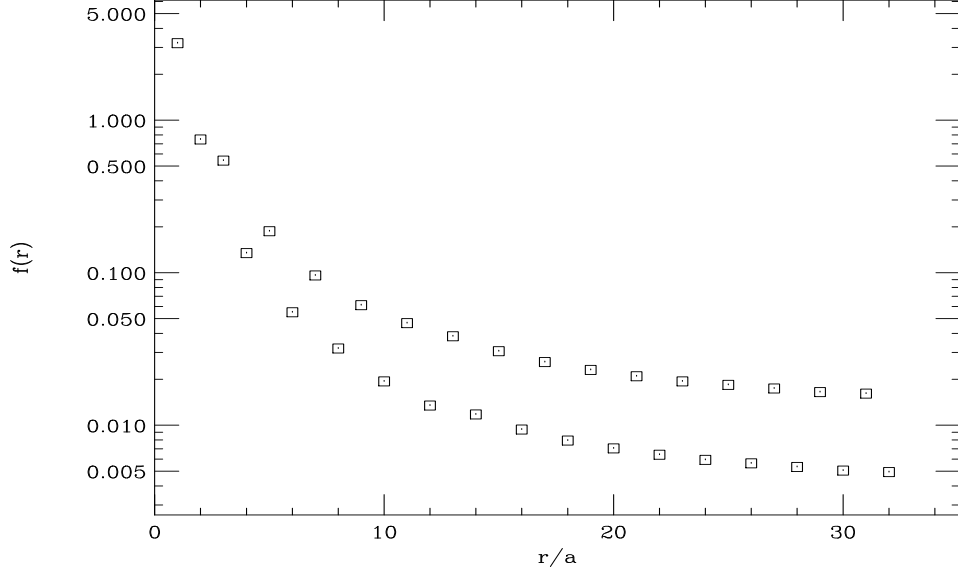


FIG. 1: Probe of the range of the \mathcal{D} operator, Eq. (3.11). The value of f at $r = 0$ is zero and is not shown in this plot. Even r are consistently lower than odd r .

We show this function for a 16^4 lattice in Fig. 1. What one sees is that there is a long tail on the operator. In contrast to the overlap operator, we do not find exponential localization; the localization that does occur is less pronounced and we view it as an open question whether or not this is harmful.

C. Tilde/untilde equivalence

Suppose we wish to compute correlation functions of the untilde fields. For this purpose we introduce sources that couple only to them:

$$S_{src} = -a^4 \sum_x \left\{ \eta^T C P_+ \chi + \tau^T C P_- \chi + J^* \phi + J \phi^* + k^* F + k F^* \right\} \quad (3.12)$$

Next we integrate out the auxiliary fields X, Φ, \mathcal{F} . The corresponding equations of motion, determined by variation of X, Φ, \mathcal{F} holding $\tilde{\chi}, \tilde{\phi}, \tilde{F}$ constant, involve the sources. These can then be solved for the auxiliary fields X, Φ, \mathcal{F} :

$$\begin{aligned} X &= -\frac{a}{2} \left(1 - \frac{a}{2} D \right)^{-1} [D \tilde{\chi} + P_+ \eta + P_- \tau] \\ \Phi &= -\frac{a}{2} \left(1 - \frac{a}{2} D_2 \right)^{-1} \tilde{F}^* - \frac{a}{2} k^* - \frac{a^2}{4} \left(1 - \frac{a}{2} D_2 \right)^{-1} J \\ \mathcal{F} &= D_2 \tilde{\phi}^* + \frac{a}{2} D_2 k - \frac{a}{2} J \end{aligned} \quad (3.13)$$

Thus when these are used to eliminate X, Φ, \mathcal{F} , quadratic terms in the sources are generated. We obtain

$$\begin{aligned}
S + S_{src} = & -a^4 \sum_x \left\{ \frac{1}{2} \tilde{\chi}^T C \left(1 - \frac{a}{2} D\right)^{-1} D \tilde{\chi} - \frac{2}{a} \tilde{\phi}^* D_2 \tilde{\phi} + \tilde{F}^* \left(1 - \frac{a}{2} D_2\right)^{-1} \tilde{F} \right. \\
& + \frac{1}{2} \tilde{\chi}^T \left(m P_+ + m^* P_- + 2g \tilde{\phi} P_+ + 2g^* \tilde{\phi}^* P_- \right) \tilde{\chi} \\
& + \tilde{F}^* (m^* \tilde{\phi}^* + g^* \tilde{\phi}^{*2}) + \tilde{F} (m \tilde{\phi} + g \tilde{\phi}^2) \\
& + \frac{a}{4} (\eta^T P_+ + \tau^T P_-) C \left(1 - \frac{a}{2} D\right)^{-1} (P_+ \eta + P_- \tau) \\
& + (\eta^T P_+ + \tau^T P_-) C \left(1 - \frac{a}{2} D\right)^{-1} \tilde{\chi} + k (\tilde{F}^* - D_2 \tilde{\phi} + \frac{a}{2} J) \\
& + k^* (\tilde{F} - D_2 \tilde{\phi}^* + \frac{a}{2} J^*) + J \tilde{\phi}^* + J^* \tilde{\phi} - \frac{a}{2} k^* D_2 k \\
& + \frac{a}{2} \tilde{F} \left(1 - \frac{a}{2} D_2\right)^{-1} J + \frac{a}{2} \tilde{F}^* \left(1 - \frac{a}{2} D_2\right)^{-1} J^* - \frac{a^2}{4} (J J + J^* J^*) \\
& \left. + \frac{a^2}{4} J^* \left(1 - 2a D_2 + \frac{a^2}{4} (D_1^2 + D_2^2)\right) \left(1 - \frac{a}{2} D_2\right)^{-2} J \right\} \quad (3.14)
\end{aligned}$$

As far as the source terms for the elementary fields χ and ϕ are concerned, working with the tilded fields is the same as working with the untilded fields up to $\mathcal{O}(a)$ corrections. Note however that the source terms involving k, k^* have unusual terms that do not vanish in the continuum limit. The implication is that correlation functions for F, F^* differ from those of \tilde{F}, \tilde{F}^* in a way that is guaranteed not to vanish in the continuum limit.

To see what are the implications for the physical fields, we set $k = k^* = 0$ and integrate out the auxiliary fields \tilde{F}, \tilde{F}^* :

$$\begin{aligned}
S + S_{src} = & -a^4 \sum_x \left\{ \frac{1}{2} \tilde{\chi}^T C \left(1 - \frac{a}{2} D\right)^{-1} D \tilde{\chi} - \frac{2}{a} \tilde{\phi}^* D_2 \tilde{\phi} \right. \\
& + \frac{1}{2} \tilde{\chi}^T \left(m P_+ + m^* P_- + 2g \tilde{\phi} P_+ + 2g^* \tilde{\phi}^* P_- \right) \tilde{\chi} \\
& + (m^* \tilde{\phi}^* + g^* \tilde{\phi}^{*2}) \left(1 - \frac{a}{2} D_2\right) (m \tilde{\phi} + g \tilde{\phi}^2) \\
& + \frac{a}{4} (\eta^T P_+ + \tau^T P_-) C \left(1 - \frac{a}{2} D\right)^{-1} (P_+ \eta + P_- \tau) \\
& + (\eta^T P_+ + \tau^T P_-) C \left(1 - \frac{a}{2} D\right)^{-1} \tilde{\chi} \\
& + \left[J^* \left(\tilde{\phi} - \frac{a}{2} (m \tilde{\phi} + g \tilde{\phi}^2) \right) + \text{h.c.} \right] - \frac{a^2}{4} (J^2 + J^{*2}) \\
& \left. - \frac{a^3}{2} J^* \left(D_2 - \frac{a^2}{8} (D_1^2 + D_2^2) \right) \left(1 - \frac{a}{2} D_2\right)^{-2} J \right\} \quad (3.15)
\end{aligned}$$

To interpret this result, suppose instead we had introduced sources $\tilde{J}, \tilde{J}^*, \tilde{\eta}, \tilde{\tau}$ for the tilded fields $\tilde{\phi}^*, \tilde{\phi}, P_+ \tilde{\chi}, P_- \tilde{\chi}$:

$$S_{src} = -a^4 \sum_x \left\{ \tilde{\eta}^T C P_+ \tilde{\chi} + \tilde{\tau}^T C P_- \tilde{\chi} + \tilde{J}^* \tilde{\phi} + \tilde{J} \tilde{\phi}^* \right\} \quad (3.16)$$

From (3.15) what we see is that

$$\frac{\delta}{\delta J(x)} = \frac{\delta}{\delta \tilde{J}(x)} + \mathcal{O}(a) \quad (3.17)$$

and likewise for the other sources $\tilde{J}^*, \tilde{\eta}, \tilde{\tau}$. This is another way of saying that the correlation functions for the tilded fields are equal to the correlation functions of the untilded fields, up to $\mathcal{O}(a)$ corrections. Of course if there were $\mathcal{O}(1/a)$ or worse divergences in the correlation functions, then the difference between the two sets of correlation functions does not vanish in the continuum limit. However, what we will find below is that at one loop the divergences are only $\ln a$, hence the tilded and untilded correlation functions become equal in the continuum limit. If $\mathcal{O}(1/a)$ or worse divergences appear at higher orders, then the two formulations are not equivalent in the continuum limit. In that case one is free to choose one or the other as the subject for fine-tuning in order to approach the continuum theory. We will choose the tilded formulation in our work.

D. Naive continuum limit

For reference, we state the basic properties of the lattice theory that guarantee that the correct continuum limit is achieved classically. Two useful identities involving the lattice derivative operators are

$$\lim_{a \rightarrow 0} D_1 = \not{\partial}, \quad \lim_{a \rightarrow 0} \frac{2}{a} D_2 = -\square \quad (3.18)$$

Then in the naive continuum limit

$$\left(1 - \frac{a}{2} D_2\right)^{-1} \rightarrow \left(1 + \frac{a^2}{4} \square\right)^{-1} \rightarrow 1 \quad (3.19)$$

Thus we see that for the kinetic terms

$$\begin{aligned} & a^4 \sum_x \left\{ \frac{1}{2} \tilde{\chi}^T C \left(1 - \frac{a}{2} D_2\right)^{-1} D_1 \tilde{\chi} - \frac{2}{a} \tilde{\phi}^* D_2 \tilde{\phi} + \tilde{F}^* \left(1 - \frac{1}{2} a D_2\right)^{-1} \tilde{F} \right\} \\ & \rightarrow \int d^4x \left\{ \frac{1}{2} \tilde{\chi}^T C \not{\partial} \tilde{\chi} + \tilde{\phi}^* \square \tilde{\phi} + \tilde{F}^* \tilde{F} \right\} \end{aligned} \quad (3.20)$$

It is interesting that the continuum limit of the action written in terms of the tilded fields is correct. This is a further indication that we can just as well treat them as the ‘‘physical’’ variables and work entirely in terms of the action (2.17).

IV. ONE-LOOP CALCULATION

In [1] an identical calculation is performed, in that they also compute one-loop corrections to the propagators and proper vertices. The action that they use, described by

their Eq. (2.17), is different from the one employed here, but is related by a singular field transformation [2]. We have confirmed the results of [1], working in this alternative but perturbatively equivalent formulation. Our results also lead to conclusions identical to those of [5], who take a different approach to studying the same action as the one we use, our Eq. (2.17); they study the counterterms that must be added to the action in order for the restoration of the supersymmetry Ward-Takahashi identity to occur.

A. Definitions

Throughout our presentation, we make use of

$$P_\mu(k) \equiv a^{-1} \sin(k_\mu a), \quad Q_\mu(k) \equiv 2a^{-1} \sin(k_\mu a/2), \quad (4.1)$$

periodic functions that reduce to momentum in the naive continuum limit. It is also useful to define

$$M(k) = 1 - 2 \sum_\mu \sin^2(k_\mu a/2) = 1 - \frac{a^2}{2} Q^2(k), \quad s(k) = \sqrt{P^2(k)a^2 + M^2(k)} \quad (4.2)$$

which has the property $\lim_{a \rightarrow 0} s(k) = 1$.

B. Analytic results

The only nonvanishing one-loop scalar two-point function is the one that gives a one-loop correction to the nonholomorphic term in the effective action,

$$\int d^4x d^4y \tilde{\phi}^*(x) G_{\tilde{\phi}^* \tilde{\phi}}^{-1}(x, y) \tilde{\phi}(y) \quad (4.3)$$

where $G(x, y)$ is the scalar propagator. It is obtained from the sum of the two diagrams shown in Fig. 2, yielding:

$$a^2 |g|^2 \int_{-\pi/a}^{\pi/a} \frac{d^4k}{(2\pi)^4} \frac{N(k, p)}{D(k, p)}, \quad N(k, p) = \frac{n(k, p)}{d(k, p)} - t(k) \quad (4.4)$$

$$n(k, p) = a^2 P(p+k) \cdot P(k), \quad d(k, p) = s(k)s(k+p), \quad t(k) = \frac{P^2(k)a^2}{s^2(k)} \quad (4.5)$$

$$D(k, p) = r(k)r(k+p), \quad r(k) = 2 \left(1 - \frac{M(k)}{s(k)} \right) + \frac{|m|^2 a^2}{2} \left(1 + \frac{M(k)}{s(k)} \right) \quad (4.6)$$

The result vanishes at $p = 0$, because $N(k, 0) = 0$, so no mass counterterm arises from this diagram.

It is interesting that a term in the effective action of the form

$$\int d^4x d^4y \tilde{\phi}(x) G_{\tilde{\phi}\tilde{\phi}}^{-1}(x, y) \tilde{\phi}(y) \quad (4.7)$$

is not generated at one-loop, since it is allowed by the symmetries of the lattice action if $m \neq 0$ and $g \neq 0$. At one-loop there is an exact cancellation between the scalar and fermion loops for all external momentum p .

The diagram that corrects the fermion propagator, Fig. 3, is given by:

$$(-i)|g|^2 \int \frac{a^4 d^4k}{(2\pi)^4} P_- \frac{\mathcal{P}(p+k)}{r(k)r(p+k)s(p+k)} \quad (4.8)$$

The diagram Fig. 4 gives the correction to the $\tilde{F}^* \tilde{F}$ term and is given by:

$$(-1)|g|^2 \int \frac{a^4 d^4k}{(2\pi)^4} \frac{1}{r(k)r(p+k)} \quad (4.9)$$

The 3-point diagram shown in Fig. 5 evaluates to:

$$\frac{-im|g|^2 g^*}{2a} \int \frac{a^4 d^4k}{(2\pi)^4} \frac{\mathcal{P}(p'+k) (1 + M(p+k)/s(p+k))}{r(p'+k)r(p+k)r(k)s(p'+k)} P_- \quad (4.10)$$

Note that when the external momenta are set to $p = p' = 0$, this expression vanishes, due to an odd integrand, $\mathcal{P}(-k) = -\mathcal{P}(k)$. Thus the Yukawa coupling receives no corrections in the zero-momentum subtraction scheme.

The $Z - 1$ counterterms (cf. Eq. (4.16) below) are computed in the usual way, from the sum of amputated one-particle irreducible self energy diagrams $\Sigma(p)$. For instance in the case of the scalar

$$\langle \tilde{\phi}(p) \tilde{\phi}^*(p) \rangle = \frac{1}{p^2 + m^2} + \frac{1}{p^2 + m^2} \Sigma(p) \frac{1}{p^2 + m^2} - \frac{1}{p^2 + m^2} (Z_\phi - 1) p^2 \frac{1}{p^2 + m^2} + \dots \quad (4.11)$$

where \dots represents higher order terms. Since there is no mass renormalization at one loop we have $\Sigma(0) = 0$ and $\Sigma(p) \equiv |g|^2 \Sigma_2 p^2 + \mathcal{O}(p^4)$. So, to have cancellation of Σ_2 at $p = 0$ we require $Z_\phi - 1 = |g|^2 \Sigma_2$.

C. Numerical results

We have computed the loop integrals in two ways: working with discrete sums at finite system size L , and with numerical integration for infinite system size $L \rightarrow \infty$. We set the scale using the bare mass m . In the discrete sums, we use $mL = 8$; the number of lattice sites in any direction is $N = L/a = mL/ma$. Equivalently, $ma = mL/N$ determines the lattice spacing in units of m . We have also computed with $mL = 16$ and find that the difference is only in the third or fourth significant figure. For the scalar we compute $Z_\phi - 1 = \lim_{p \rightarrow 0} \Sigma_\phi(p)/p^2$, with $\Sigma_\phi(p)$ the one-loop self-energy Fig. 2, since $\Sigma(p)$ vanishes



FIG. 2: Scalar 2-point function that contributes to self-energy.

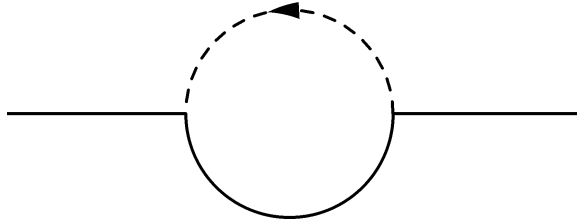


FIG. 3: Fermion 2-point function that contributes to self-energy.

at $p = 0$, as noted above. The results are given in Table I. For the fermion we compute $Z_\chi - 1 = \lim_{p \rightarrow 0} \Sigma_\chi(\not{p})/\not{p}$ since $\Sigma_\chi(\not{p})$ vanishes at $\not{p} = 0$. The results are given in Table II. For the auxiliary field, we compute $Z_F - 1 = \Sigma_F(0)$. The results are given in Table III.

We have fit the $L = \infty$ numerical data with $ma \leq 0.125$ to

$$f(ma) = c_0 \ln(ma) + c_1 ma + c_2 (ma)^2 \quad (4.12)$$

Giving the data points equal weight, the fit for the scalar self energy is

$$c_0 = 0.00604(7), \quad c_1 = 0.024(20), \quad c_2 = -0.15(17) \quad (4.13)$$

while for the fermion the fit is

$$c_0 = 0.00597(5), \quad c_1 = 0.061(15), \quad c_2 = -0.39(12) \quad (4.14)$$

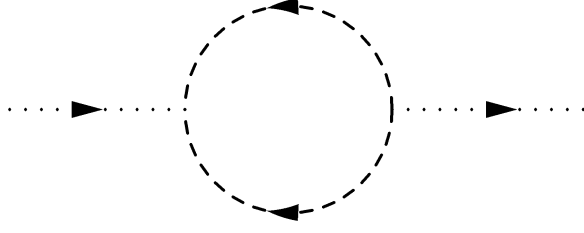


FIG. 4: Auxiliary 2-point function that contributes to self-energy.

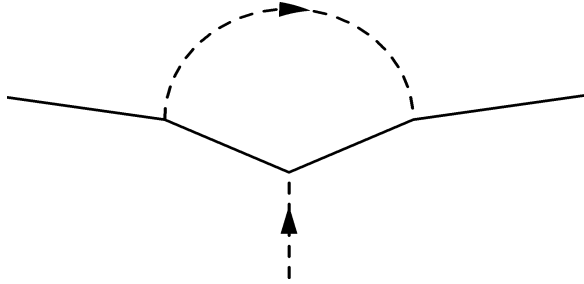


FIG. 5: 3-point function.

Thus we see that at $L \rightarrow \infty$ the log divergences of the scalar $Z_\phi - 1$ and the fermion $Z_\chi - 1$ match. For the auxiliary field we obtain instead

$$c_0 = -0.0261(5), \quad c_1 = 0.87(11), \quad c_2 = -3.9(1.0) \quad (4.15)$$

so that its $Z_F - 1$ does not match the scalar and fermion. This is consistent with the results found in [5].

D. Renormalization

We can absorb all the logarithmic divergence by rescaling the fields, so that the action is modified from (2.17) and (2.19) to read

$$\begin{aligned} S &= -a^4 \sum_x \left\{ \frac{1}{2} Z_\chi \tilde{\chi}^T C M \tilde{\chi} - Z_\phi \tilde{\phi}^* D_2 \tilde{\phi} + Z_F \tilde{F}^* (1 - \frac{a}{2} D_2)^{-1} \tilde{F} \right. \\ &\quad \left. + \sqrt{Z_F} \tilde{F}^* (m^* \sqrt{Z_\phi} \tilde{\phi}^* + g^* Z_\phi \tilde{\phi}^{*2}) + \sqrt{Z_F} \tilde{F} (m \sqrt{Z_\phi} \tilde{\phi} + g Z_\phi \tilde{\phi}^2) \right\}, \\ M &= \mathcal{D} + (m + 2g \sqrt{Z_\phi} \tilde{\phi}) P_+ + (m^* + 2g^* \sqrt{Z_\phi} \tilde{\phi}^*) P_-, \\ \mathcal{D} &= (1 - \frac{1}{2} a D_2)^{-1} D_1 \end{aligned} \quad (4.16)$$

ma	$(Z-1)(\infty)/ g ^2$	$(Z-1)(8)/ g ^2$
0.5	-0.00589	-0.006355
0.25	-0.00884	-0.009532
0.125	-0.01205	-0.013358
0.0625	-0.01573	-0.017541
0.03125	-0.01986	-0.021837
0.015625	-0.02573	-0.026205
0.0078125	-0.02956	-0.030583
0.00390625	-0.03370	—
0.001953125	-0.03671	—

TABLE I: Self-energy for the scalar, from Fig. 2 evaluated at $p = (0, 0, 0, 2\pi/L)$ for $L = \infty$ and $mL = 8$.

ma	$(Z-1)(\infty)/ g ^2$	$(Z-1)(8)/ g ^2$
0.5	-0.00385	-0.004027
0.25	-0.00715	-0.006973
0.125	-0.01085	-0.011406
0.0625	-0.01463	-0.015632
0.03125	-0.01893	-0.019965
0.015625	-0.02319	-0.024336
0.007813	-0.02910	-0.028720
0.00390625	-0.03311	—
0.001953125	-0.03697	—

TABLE II: One-loop counterterm $Z-1$ for the fermion, evaluated from slope in self-energy in $p \rightarrow 0$ limit, for $L = \infty$ and $mL = 8$. Note that the lattice spacing is measured in units of $1/m$.

It is interesting that when one eliminates \tilde{F}, \tilde{F}^* by their equations of motion, the constant Z_F disappears entirely:

$$S = -a^4 \sum_x \left\{ \frac{1}{2} Z_\chi \tilde{\chi}^T C M \tilde{\chi} - Z_\phi \tilde{\phi}^* D_2 \tilde{\phi} - (m^* \sqrt{Z_\phi} \tilde{\phi}^* + g^* Z_\phi \tilde{\phi}^{*2}) (1 - \frac{a}{2} D_2) (m \sqrt{Z_\phi} \tilde{\phi} + g Z_\phi \tilde{\phi}^2) \right\}, \quad (4.17)$$

The discrepancy between Z_F and $Z_\chi = Z_\phi$ is irrelevant to the physical theory, which only contains $\tilde{\phi}$ and $\tilde{\chi}$. In terms of the on-shell formulation, the one-loop renormalization of the lattice theory, in the $a \rightarrow 0$ limit, exactly mirrors what occurs in the continuum theory. The mismatch $Z_F \neq Z_\chi = Z_\phi$ will have effects at two loops, where one-loop corrected

ma	$(Z-1)(\infty)/ g ^2$	$(Z-1)(8)/ g ^2$
0.5	0.100785	0.082542
0.25	0.0994727	0.088658
0.125	0.103388	0.095266
0.0833333	0.106955	0.09916
0.0625	0.10983	0.105719
0.03125	0.117483	0.11255
0.015625	0.125715	0.13276
0.0078125	0.134227	0.140261
0.00390625	0.14287365	0.147476

TABLE III: Self-energy for the auxiliary field, evaluated at $p = 0$ for $L = \infty$ and $mL = 8$.

propagators will be involved in subdiagrams. Cancellations that in the continuum make use of equalities of counterterms will no longer hold. Thus we expect that nonsupersymmetric renormalization of the on-shell formulation first appears at two loops.

E. Locality

As stated above, we have computed $Z_\phi - 1 = \lim_{p \rightarrow 0} \Sigma_\phi(p)/p^2$. The fact that this has a finite limit demonstrates that at small p , the self-energy is analytic in p^2 . Thus we find that

$$\Sigma_\phi(p) = \Sigma_2 p^2 + \mathcal{O}(p^4) \quad (4.18)$$

and there is no evidence of nonlocality in the scalar self-energy.

V. SUPERCURRENT, MIXING AND RENORMALIZATION

For a general superpotential $W(\phi)$, the supercurrent is

$$S^\mu = \sqrt{2} \left[\not{\partial} \phi \gamma^\mu P_{+\chi} + \not{\partial} \phi^* \gamma^\mu P_{-\chi} + \frac{\partial W}{\partial \phi} \gamma^\mu P_{-\chi} + \left(\frac{\partial W}{\partial \phi} \right)^* \gamma^\mu P_{+\chi} \right] \quad (5.1)$$

and in our case $\partial W/\partial \phi = m\phi + g\phi^2$. Because of the supersymmetry breaking on the lattice, this will mix with other operators in the same symmetry channel. For example, one has at the same naive dimension the operator

$$T^\mu = \partial^\mu \phi^* P_{-\chi} + \partial^\mu \phi P_{+\chi} \quad (5.2)$$

If the lattice action (Eq. (2.22) in the massive case and Eq. (2.23) in the massless case) is fine-tuned, then in the long distance effective theory there will be a supercurrent that is

conserved in the continuum limit. Thus one way to detect supersymmetry is to consider linear combinations of bare lattice operators and extract the one that has vanishing four-divergence in the supersymmetric limit, modulo contact terms. We will study that approach in Section VD below. Before doing so, we briefly consider a naive discretization of the continuum supercurrent (5.1).

A. Naive lattice supercurrent

We formulate this lattice supercurrent in terms of tilded fields:

$$\begin{aligned} S^\mu &= \sqrt{2} \left[D_1 \tilde{\phi} \gamma^\mu P_+ \tilde{\chi} + D_1 \tilde{\phi}^* \gamma^\mu P_- \tilde{\chi} + \frac{\partial W}{\partial \tilde{\phi}} \gamma^\mu P_- \tilde{\chi} + \left(\frac{\partial W}{\partial \tilde{\phi}} \right)^* \gamma^\mu P_+ \tilde{\chi} \right] \\ \frac{\partial W}{\partial \tilde{\phi}} &= m \tilde{\phi} + g \tilde{\phi}^2 \end{aligned} \quad (5.3)$$

For instance the correlation functions

$$\langle S_\mu(x) \tilde{\phi}(y) \tilde{\chi}(0) C \rangle, \quad \langle S_\mu(x) \tilde{\phi}^*(y) \tilde{\chi}(0) C \rangle \quad (5.4)$$

give rise to tree-level diagrams from the quadratic terms in S^μ . It is straightforward to obtain at this order

$$\langle S_\mu(x) \tilde{\phi}(y) \tilde{\chi}(0) C \rangle = \sqrt{2} \gamma_\nu \gamma_\mu P_- S(x) D_{1\nu}^{(x)} G(y-x) + \sqrt{2} m^* \gamma_\mu P_+ S(x) G(y-x) \quad (5.5)$$

where $S(x) = \langle \tilde{\chi}(x) \tilde{\chi}(0) C \rangle$ is the free theory fermion propagator and $G(x) = \langle \tilde{\phi}(x) \tilde{\phi}^*(0) \rangle$ is the free theory scalar propagator. This will have the correct continuum limit $\partial_\mu S_\mu = 0$, modulo contact terms, since no divergences appear at tree-level. This can be explicitly checked by differentiating the expression above and using the equations satisfied by the free propagators:

$$\begin{aligned} D_1 S(x) &= -(m P_+ + m^* P_-) S(x) + \mathcal{O}(a), \quad x \neq 0 \\ D_1 D_1 G(x) &= |m|^2 G(x) + \mathcal{O}(a), \quad x \neq 0 \end{aligned} \quad (5.6)$$

The variation of the action under the lattice version of the supersymmetry transformation (2.14) and (2.15) is

$$\delta S = \sqrt{2} a^4 \sum_x \tilde{\chi}^T C \left[g P_+ (2 \tilde{\phi} D_1 \tilde{\phi} - D_1 \tilde{\phi}^2) + g^* P_- (2 \tilde{\phi}^* D_1 \tilde{\phi}^* - D_1 \tilde{\phi}^{*2}) \right] \epsilon \quad (5.7)$$

Note that this is $\mathcal{O}(a)$, since

$$\lim_{a \rightarrow 0} \sum_x \tilde{\chi}^T C P_+ (2 \tilde{\phi} D_1 \tilde{\phi} - D_1 \tilde{\phi}^2) = 0 \quad (5.8)$$

Also note the presence of g in (5.7). In order to see violation of the supersymmetric identity $\partial_\mu S_\mu = 0$ in the continuum limit, diagrams involving the coupling g must be included. Loop diagrams are required, in order to get the divergences that cancel the $\mathcal{O}(a)$ factor coming from (5.7) in the continuum limit.

B. Exactly conserved supercurrent?

Because of (5.7), one can ask whether in the $g = 0$ limit there is an exactly conserved supercurrent; by a proper latticization of the continuum supercurrent and the four-divergence, we would hope to find a discretized version of $\partial_\mu S_\mu = 0$ that holds at finite lattice spacing. In order to search for this hypothetical supercurrent, we follow the usual method and suppose that the parameter of the transformation ϵ depends on spacetime position, $\epsilon = \epsilon(x)$. Variation of the action with site-dependent ϵ can generally be written in the form:

$$\Delta S = -a^4 \sum_x \epsilon^T(x) C \mathfrak{S}(x) \quad (5.9)$$

Thus in the form of the action with all fields, Eq. (2.10),

$$\begin{aligned} \mathfrak{S} &= -\frac{1}{a^4} \frac{\delta S}{\delta(\epsilon^T C)} \\ &= -\sqrt{2}(D_1\phi D_1 P_{-\chi} + D_1^2\phi P_{-\chi} + D_1\phi D_2 P_{+\chi} + D_2\phi D_1 P_{+\chi} \\ &\quad + D_1\phi^* D_1 P_{+\chi} + D_1^2\phi^* P_{+\chi} + D_1\phi^* D_2 P_{-\chi} + D_2\phi^* D_1 P_{-\chi} \\ &\quad + D_2 F P_{+\chi} - F D_2 P_{+\chi} + D_2 F^* P_{-\chi} - F^* D_2 P_{-\chi}) \\ &\quad -\sqrt{2}m(D_1\tilde{\phi} P_{+\tilde{\chi}} + \tilde{\phi} D_1 P_{+\tilde{\chi}}) - \sqrt{2}m^*(D_1\tilde{\phi}^* P_{-\tilde{\chi}} + \tilde{\phi}^* D_1 P_{-\tilde{\chi}}) \\ &\quad -\sqrt{2}g(2\tilde{\phi} D_1\tilde{\phi} P_{+\tilde{\chi}} + \tilde{\phi}^2 D_1 P_{+\tilde{\chi}}) - \sqrt{2}g^*(2\tilde{\phi}^* D_1\tilde{\phi}^* P_{-\tilde{\chi}} + \tilde{\phi}^{*2} D_1 P_{-\tilde{\chi}}) \\ &\quad + \frac{2}{a}\sqrt{2}(D_1\Phi P_{+X} + \Phi D_1 P_{+X} + D_1\Phi^* P_{-X} + \Phi^* D_1 P_{-X}) \end{aligned} \quad (5.10)$$

On the other hand, when we just work with tilded fields, Eq. (2.17),

$$\begin{aligned} \mathfrak{S} &= -\sqrt{2}(D_1\tilde{\phi} \mathbb{D} P_{-\tilde{\chi}} - \tilde{F} \mathbb{D} P_{-\tilde{\chi}} + D_1\tilde{\phi}^* \mathbb{D} P_{+\tilde{\chi}} - \tilde{F}^* \mathbb{D} P_{+\tilde{\chi}}) \\ &\quad + \sqrt{2}\left(\frac{2}{a}D_2\tilde{\phi} P_{-\tilde{\chi}} + \frac{2}{a}D_2\tilde{\phi}^* P_{+\tilde{\chi}}\right) \\ &\quad -\sqrt{2}(D_1 P_{-\tilde{\chi}}(1 - \frac{a}{2}D_2)^{-1}\tilde{F} + D_1 P_{+\tilde{\chi}}(1 - \frac{a}{2}D_2)^{-1}\tilde{F}^*) \\ &\quad -\sqrt{2}m(D_1\tilde{\phi} P_{+\tilde{\chi}} + \tilde{\phi} D_1 P_{+\tilde{\chi}}) - \sqrt{2}m^*(D_1\tilde{\phi}^* P_{-\tilde{\chi}} + \tilde{\phi}^* D_1 P_{-\tilde{\chi}}) \\ &\quad -\sqrt{2}g(2\tilde{\phi} D_1\tilde{\phi} P_{+\tilde{\chi}} + \tilde{\phi}^2 D_1 P_{+\tilde{\chi}}) - \sqrt{2}g^*(2\tilde{\phi}^* D_1\tilde{\phi}^* P_{-\tilde{\chi}} + \tilde{\phi}^{*2} D_1 P_{-\tilde{\chi}}) \end{aligned} \quad (5.11)$$

Finally, for the quadratic terms there exist lattice identities analogous to integration by parts, such as:

$$\sum_x D_1\phi D_1 P_{-\chi} = -\sum_x \phi D_1^2 P_{-\chi}, \quad \sum_x D_2\phi D_1 P_{+\chi} = \sum_x \phi D_1 D_2 P_{+\chi} \quad (5.12)$$

These sorts of identities give us, for either form of \mathfrak{S} ,

$$\begin{aligned} \sum_x a^4 \mathfrak{S} &= -\sqrt{2} \sum_x a^4 \left\{ g(2\tilde{\phi} D_1\tilde{\phi} P_{+\tilde{\chi}} + \tilde{\phi}^2 D_1 P_{+\tilde{\chi}}) \right. \\ &\quad \left. g^*(2\tilde{\phi}^* D_1\tilde{\phi}^* P_{-\tilde{\chi}} + \tilde{\phi}^{*2} D_1 P_{-\tilde{\chi}}) \right\} \end{aligned} \quad (5.13)$$

In the continuum limit this quantity also vanishes; however, on the lattice we cannot integrate this cubic quantity by parts and the expression inside braces gives an $\mathcal{O}(a)$ deviation from zero.

In conclusion we do not find an exactly conserved supercurrent at $g = 0$ but we do find an expression for which $\sum_x \mathfrak{S} = 0$, behaving as if $\mathfrak{S} \sim \partial_\mu S_\mu$, for $g = 0$. The quantity \mathfrak{S} will play an important role in the broken supersymmetry Ward-Takahashi identities of the lattice theory, which we consider next.

C. Broken Ward-Takahashi identities

As we have just seen, the variation of the action under an x -dependent spinor parameter $\epsilon_\alpha(x)$ cannot be written as a simple product of ϵ and a finite difference operator acting on an expression like (5.3). Otherwise (5.13) would vanish. Rather, it takes a more general form, which we have denoted above as (5.9). Thus \mathfrak{S} will appear in the broken Ward-Takahashi identities that we are about to derive. Parenthetically, in the classical continuum limit, with the discretization (5.3) of the supercurrent,

$$\lim_{a \rightarrow 0} (\mathfrak{S}_\alpha(x) - \partial_\mu S_{\mu,\alpha}(x)) = 0 \quad (5.14)$$

because we know that each term should go over to the continuum expression $\partial_\mu S_{\mu,\alpha}(x)$.

In addition to (5.9), we also must consider the variation of the source terms,

$$S_{src} = -a^4 \sum_x \left\{ \tilde{\eta}^T C P_+ \tilde{\chi} + \tilde{\tau}^T C P_- \tilde{\chi} + \tilde{J}^* \tilde{\phi} + \tilde{J} \tilde{\phi}^* + \tilde{k}^* \tilde{F} + \tilde{k} \tilde{F}^* \right\} \quad (5.15)$$

For this purpose we define $\delta_\epsilon \tilde{\phi} = (\epsilon^T C)_\alpha \Delta_\alpha \tilde{\phi}$, etc. The supersymmetry transformations of the tilded fields are given in (2.16). Thus

$$\begin{aligned} \Delta_\alpha \tilde{\chi}_\beta &= -\sqrt{2}(P_+(D_1 \tilde{\phi} + \tilde{F})C)_{\beta\alpha} - \sqrt{2}(P_-(D_1 \tilde{\phi}^* + \tilde{F}^*)C)_{\beta\alpha}, \\ \Delta_\alpha \tilde{\phi} &= \sqrt{2}(P_+ \tilde{\chi})_\alpha, \quad \Delta_\alpha \tilde{\phi}^* = \sqrt{2}(P_- \tilde{\chi})_\alpha \\ \Delta_\alpha \tilde{F} &= \sqrt{2}(D_1 P_+ \tilde{\chi})_\alpha, \quad \Delta_\alpha \tilde{F}^* = \sqrt{2}(D_1 P_- \tilde{\chi})_\alpha \end{aligned} \quad (5.16)$$

Then we have the identity

$$\begin{aligned} \Delta_\alpha Z(\mathcal{J}; x) = 0 &= \int [d\tilde{\phi} d\tilde{\phi}^* d\tilde{\chi} d\tilde{F} d\tilde{F}^*] e^{-S - S_{src}} \left[\mathfrak{S}_\alpha(x) \right. \\ &+ (\tilde{\eta}^T C P_+ \Delta_\alpha \tilde{\chi})(x) + (\tilde{\tau}^T C P_- \Delta_\alpha \tilde{\chi})(x) \\ &\left. + (\tilde{J}^* \Delta_\alpha \tilde{\phi})(x) + (\tilde{J} \Delta_\alpha \tilde{\phi}^*)(x) + (\tilde{k}^* \Delta_\alpha \tilde{F})(x) + (\tilde{k} \Delta_\alpha \tilde{F}^*)(x) \right] \end{aligned} \quad (5.17)$$

Here \mathcal{J} collectively denotes all the sources and S is the action (2.17). Since the identity holds for all values of \mathcal{J} , derivatives of $\Delta Z(\mathcal{J}; x)$ with respect to the sources also vanish.

Thus it is the generating function of lattice correlation function identities associated with the supersymmetry transformations (2.16). We refer to these as the broken supersymmetry Ward-Takahashi identities.

We could measure a lattice transcription of the Ward-Takahashi identities that vanish in the continuum theory. Their deviation from zero gives a measure of the amount of supersymmetry violation in the latticized theory. A simple example is the following.

$$\begin{aligned} & \left(\frac{\delta}{\delta(\tilde{\eta}^T C)_\beta(y)} + \frac{\delta}{\delta(\tilde{\tau}^T C)_\beta(y)} \right) \Delta_\alpha Z(\mathcal{J}, x) \Big|_{\mathcal{J}=0} = 0 \\ & = \langle -a^4 \mathfrak{S}_\alpha(x) \tilde{\chi}_\beta(y) - \sqrt{2}((D_1 \tilde{\phi} + \tilde{F})C)_{\beta\alpha}(x) \delta(x, y) \rangle \end{aligned} \quad (5.18)$$

This leads us to the identity

$$\sqrt{2} \sum_x a^4 \langle \tilde{F}(x) \rangle C_{\alpha\beta} = - \sum_{x,y} a^8 \langle \mathfrak{S}_\alpha(x) \tilde{\chi}_\beta(y) \rangle \quad (5.19)$$

In the continuum theory the right-hand side vanishes because $\mathfrak{S} \rightarrow \partial_\mu S_\mu$. On the lattice we have instead the simplified expression (5.13), which is an $\mathcal{O}(a)$ lattice artifact. Divergent behavior in $\langle \mathfrak{S}_\alpha(x) \tilde{\chi}_\beta(y) \rangle$ can lead to a result which does not vanish in the continuum limit. We can measure the violation of the continuum supersymmetry Ward-Takahashi identity $\int d^4x \langle F(x) \rangle = 0$ by computing either side of (5.19) in our numerical simulations. This is done for the left-hand side in Section VII D below.

Consider again the most general lattice action consistent with symmetries, Eq. (2.22). By tuning the parameters in this bare action we expect to obtain the supersymmetric limit for the long distance effective theory. On the other hand, once this fine-tuning is performed the bare lattice action (2.22) will not be invariant with respect to the supersymmetry transformation of the bare fields:

$$\delta S = -a^4 \epsilon^T C \sum_x \mathfrak{S} \neq 0 \quad (5.20)$$

Thus we continue to have modified identities, (5.17), which do not look qualitatively different from those away from the supersymmetric point in parameter space. What is different is that in the long distance effective theory there is a conserved supercurrent, $\partial_\mu S_\mu = 0$ as an operator relation in the continuum limit. To probe for supersymmetry, we must construct this supercurrent, built out of the appropriate set of bare field operators, Eq. (5.21) below.

D. Supercurrent formulation

We write down all operators that have the index structure of $S_{\mu\alpha}(x)$; leading representatives are given in Table IV. We denote these as $\mathcal{O}_{\mu\alpha,j}^{(n/2)}$ where $n/2$ is the engineering dimension. A linear combination of these is the long distance effective supercurrent at lattice

spacing a :

$$S_{\mu\alpha}(x) = \sum_{n=3,5,7,\dots} \sum_j b_j^{(n/2)}(a) a^{(n-7)/2} \mathcal{O}_{\mu\alpha,j}^{(n/2)}(x) \quad (5.21)$$

On dimensional grounds, $b_j^{(n/2)}(a)$ must be a dimensionless quantity, and is therefore a function of the renormalized parameters of the long distance theory, $m_r a$ and g_r , in the infinite volume limit. At finite volume it may also depend on a/L . We know that

$$\lim_{a \rightarrow 0} \partial_\mu S_{\mu\alpha}(x) = 0 \quad (5.22)$$

as an operator relation, provided the relevant and marginal counterterms in the lattice action (2.22) are tuned properly. If the fermion mass is set to zero, then we only need to tune the lattice action (2.23). In practice, we will add a fermion mass term to (2.23) and extrapolate to vanishing bare fermion mass.

In numerical computations it is convenient to take the spatial transform so that we instead work with

$$a^3 \sum_{\mathbf{x}} \partial_\mu S_{\mu\alpha}(t, \mathbf{x}) = a^3 \sum_{\mathbf{x}} \partial_t S_{0\alpha}(t, \mathbf{x}) = \partial_t Q_\alpha(t). \quad (5.23)$$

Since $S_{\mu\alpha}$ is fermionic, an odd number of $\tilde{\chi}$ fields must appear in nonvanishing correlation functions with $\partial_t Q_\alpha(t)$. For this reason, correlation functions should involve operators with dimension of at least $3/2$. In what follows we will exclusively consider two-point functions with fermionic operators of dimension $n/2$ which we denote $\mathcal{O}_j^{(n/2)}$, where $n = 3, 5, 7$ etc. In order to identify the supercurrent nonperturbatively, what one really wants to study is the family of correlation functions

$$M_{ij}^{(m,n)}(t) = \langle \partial_t \mathcal{O}_{0\alpha,j}^{(n/2)}(t) \mathcal{O}_i^{(m/2)}(0, \mathbf{0}) \rangle \quad (5.24)$$

where

$$\mathcal{O}_{0\alpha,j}^{(n/2)}(t) = a^3 \sum_{\mathbf{x}} \mathcal{O}_{0\alpha,j}^{(n/2)}(t, \mathbf{x}) \quad (5.25)$$

Truncating $n, m \leq N_{\max}$, we want to tune the parameters of the bare action (2.23) such that $M_{ij}^{(m,n)}(t)$ has a null space in the collective column index $B = (j, n)$ for each i, m and t , which together form a collective row index $A = (i, m, t)$:

$$\lim_{a \rightarrow 0} M_{AB} b_B = 0 \quad (5.26)$$

for all $A = 1, \dots, N_c$, with b nontrivial.

Of course at finite lattice spacing, no amount of fine-tuning will restore supersymmetry. Thus what we seek is not (5.26), but instead $M_{AB} b_B = \mathcal{O}(a)$. However we need to find b_B

dimension	operators
3/2	$\gamma_\mu P_\pm \chi$
5/2	$\gamma_\mu \phi P_\pm \chi, \gamma_\mu \phi^* P_\pm \chi, P_\pm \partial_\mu \chi, \sigma_{\mu\nu} P_\pm \partial_\nu \chi$
7/2	$\gamma_\mu \phi^2 P_\pm \chi, \gamma_\mu \phi^{*2} P_\pm \chi, \gamma_\mu \phi ^2 P_\pm \chi, \partial_\mu \phi P_\pm \chi, \partial_\mu \phi^* P_\pm \chi, \phi P_\pm \partial_\mu \chi, \phi^* P_\pm \partial_\mu \chi, \not{\partial} P_\pm \partial_\mu \chi,$ $\sigma_{\mu\nu} \partial_\nu \phi P_\pm \chi, \sigma_{\mu\nu} \partial_\nu \phi^* P_\pm \chi, \phi \sigma_{\mu\nu} \partial_\nu P_\pm \chi, \phi^* \sigma_{\mu\nu} \partial_\nu P_\pm \chi$

TABLE IV: Operators that can potentially mix with the supercurrent, up to $\mathcal{O}(a)$ suppressed higher dimensional operators.

with the constraint $\|b\| = 1$ in order to make the tuning independent of the normalization of this vector. We thus seek to minimize

$$F = \sum_A \left| \sum_B M_{AB} b_B \right|^2, \quad \sum_B |b_B|^2 \equiv 1 \quad (5.27)$$

with respect to b . This is repeated at various m_2^2 and λ_1 until the minimum is found with respect to these parameters for fixed m_1 . Finally, we make an extrapolation to $m_1 = 0$, and identify the fine-tuned pair m_2^2 and λ_1 where F approaches its minimum value.

We have taken $\|b\| = 1$ in our considerations so far. But we know that is not the whole story in the $a \rightarrow 0$ limit. The operator S_μ will undoubtedly need to be renormalized, and that will involve a divergent factor: $S_\mu^{ren.} = Z_S S_\mu$. This can be determined through a position space scheme. We demand that the free theory results are matched at some distance scale r :

$$Z_S^2 \langle S_\mu(x) S_\nu(0) \rangle_{|x|=r} = \langle S_\mu(x) S_\nu(0) \rangle_{\text{free}, |x|=r} \quad (5.28)$$

Similarly, for the operators that appear in the correlation functions with S_μ we must impose

$$(Z_i^{(m/2)})^2 \langle \mathcal{O}_i^{(m/2)}(x) \mathcal{O}_i^{(m/2)}(0) \rangle_{|x|=r} = \langle \mathcal{O}_i^{(m/2)}(x) \mathcal{O}_i^{(m/2)}(0) \rangle_{\text{free}, |x|=r} \quad (5.29)$$

Then the quantity that should be minimized, and which must vanish in the continuum limit is:

$$F = \sum_{t,m,i} \left| Z_S Z_i^{(m/2)} \sum_{j,n} b_j^{(n/2)} \langle \partial_t \mathcal{O}_{0\alpha,j}^{(n/2)}(t) \mathcal{O}_i^{(m/2)}(0, \mathbf{0}) \rangle \right|^2 \quad (5.30)$$

E. Continuum limit

Since the model is a $|\phi|^4$ theory coupled to fermions through a Yukawa interaction, it is expected to be trivial. The only continuum limit is therefore the free theory. We can work at arbitrarily small but finite lattice spacing a . Having tuned to the supersymmetric point in parameter space there is only one renormalized mass parameter m_r in the theory, and so in

lattice units we will measure $m_r a$ from the exponential decay of correlation functions of the elementary fields. Due to the $U(1)_R$ symmetry, this mass will be proportional to the bare fermion mass, which in lattice units is $m_1 a$. It follows that we take a smaller by reducing the size of the lattice parameter $m_1 a$. The triviality of the theory is then the statement that if $m_1 a = 0$, the long distance effective coupling $g_r = 0$, independently of the bare coupling y_1 (recall that λ_1 is fine-tuned to obtain the supersymmetric limit).

VI. FINE-TUNING WITH MULTICANONICAL REWEIGHTING

Multicanonical methods [20, 30, 31] combined with “Ferrenberg-Swendsen reweighting” [21–23] have proven to be a powerful tool for maximizing the usefulness of Monte Carlo simulations over a range of parameter space. We refer to this combination of techniques as multicanonical reweighting (MCRW). For instance, MCRW was applied in a study comparing $SU(2)$ and $SO(3) = SU(2)/Z_2$ lattice gauge theories [32, 33]. It was found to dramatically flatten the distributions with respect to three parameters, twists on gauge fields at the spatial boundaries. Another successful application of MCRW consists of lattice results for the electroweak phase transition [34, 35].

We will begin by describing MCRW generally for a theory of a real scalar field ϕ , followed by a presentation of how it would be applied to the lattice four-dimensional Wess-Zumino model that we are studying.

A. Preliminaries

Suppose we perform a Monte Carlo simulation at one value m_0 of the scalar mass m , so that the configurations sample the distribution determined by the action

$$S(m = m_0) = S(m = 0) + \frac{1}{2} \int d^4x m_0^2 \phi^2(x). \quad (6.1)$$

Following the “Ferrenberg-Swendsen reweighting” method [21–23] one can use the following *reweighting identity* to compute the expectation value $\langle \mathcal{O} \rangle_m$ of an operator \mathcal{O} for the distribution with a mass m :

$$\langle \mathcal{O} \rangle_m = \frac{\langle \mathcal{O} e^{-\Delta S(m)} \rangle_{m_0}}{\langle e^{-\Delta S(m)} \rangle_{m_0}} \approx \frac{\sum_{C \in F(n)} \mathcal{O}_C \exp \left[-\frac{1}{2} (m^2 - m_0^2) \int d^4x \phi_C^2 \right]}{\sum_{C \in F(n)} \exp \left[-\frac{1}{2} (m^2 - m_0^2) \int d^4x \phi_C^2 \right]}. \quad (6.2)$$

In the first equality $\langle \cdots \rangle_{m_0}$ is the expectation value with respect to the canonical distribution corresponding to (6.1) and

$$\Delta S(m) = \frac{1}{2} (m^2 - m_0^2) \int d^4x \phi^2 \quad (6.3)$$

is the shift in the action when the mass is changed. In the second, $\int d^4x \phi_C^2$ and \mathcal{O}_C are the mass term operator evaluated on configuration C and $\sum_{C \in F(n)}$ is the sum over the

distribution $F(n)$ of n configurations generated in the Monte Carlo simulation. These of course provide a finite ensemble that approximates the canonical distribution corresponding to (6.1). The advantage of this approach is that one need only perform a single simulation at mass m_0 , storing the values of $\int d^4x \phi_C^2$ and \mathcal{O}_C for each C , and then $\langle \mathcal{O} \rangle_m$ can be computed for a swath of the parameter space m without having to perform any new simulations. Typically the time for this “offline” calculation is negligible compared to that of the simulation.

Unfortunately, the regime of utility for this technique is limited by the *overlap problem*, in a way that often worsens exponentially in the spacetime volume. For instance, suppose the theory (6.1) has a quartic interaction and a critical mass-squared m_c^2 such that for $m^2 < m_c^2$ there is spontaneous symmetry breaking. If we simulate with $m_0^2 > m_c^2$ then the field is exponentially weighted toward $\int d^4x \phi^2 \approx 0$. Now suppose we attempt to reweight to $m^2 < m_c^2$. In that case $-(m^2 - m_0^2) > 0$ so that the exponential weight factor in (6.2) is minimal at $\int d^4x \phi^2 \approx 0$. The ensemble that is generated in the Monte Carlo simulation will have exponentially few configuration in the regime where $\int d^4x \phi^2$ is far from zero and $e^{-\Delta S(m)}$ is large. Because we will have very few representatives of configurations with the largest weight $e^{-\Delta S(m)}$, and most members of the ensemble have very small weight, fluctuations will be large and huge samples are required in order to have acceptable errors. The mismatch of the distributions gets worse as the number of lattice sites increases, because the exponent is extensive (i.e., scales like the spacetime volume $L^3 \times T$).

As a concrete example, Fig. 4 of [32] shows that in the range of a three-dimensional parameter space the ordinary canonical Monte Carlo density of states varies by 14 orders of magnitude. This is for an $8^3 \times 4$ lattice, which is still relatively small. The problem will get exponentially worse on larger lattices.

In a number of contexts the technique of *multicanonical reweighting* [20, 30, 31] has been found to ameliorate the overlap problem. One replaces S with

$$S_{MCRW} = S + W[\mathcal{O}_1, \mathcal{O}_2, \dots], \quad (6.4)$$

where $W[\mathcal{O}_1, \mathcal{O}_2, \dots]$ is a carefully engineered function of some small set of observables. For instance in the model that we are studying, W will be a function of the mass term and the quartic term.

$$\mathcal{O}_1 = a^4 \sum_x |\phi|^2, \quad \mathcal{O}_2 = a^4 \sum_x |\phi|^4. \quad (6.5)$$

The (reweighted) expectation value of an observable in the distribution corresponding to S_{MCRW} is:

$$\langle \mathcal{O} \rangle = \frac{\sum_{C \in F(n)} \mathcal{O}_C e^{W[\mathcal{O}_1^C, \mathcal{O}_2^C]}}{\sum_{C \in F(n)} e^{W[\mathcal{O}_1^C, \mathcal{O}_2^C]}}. \quad (6.6)$$

Since the e^W factor in (6.6) just cancels the e^{-W} Boltzmann factor coming from (6.4), one might wonder why it is introduced in the first place. The point is that the additional

Boltzmann factor e^{-W} in effect produces a weighted average over a continuum of canonical ensembles (hence the appellation “multicanonical”) such that there is a good overlap with the distribution that one is reweighting to. The challenge is to design a W such that sampling is flattened over the range of observables one is interested in.

We return to Fig. 4 of [32]. It shows that the multicanonical Monte Carlo sampling distribution is flat in the range of three-dimensional parameter space between the peaks, where the ordinary canonical Monte Carlo distribution varies by twelve orders of magnitude. The reweighting function W was represented by a numerical table, composed of the inverse density of states with respect to the tuned parameters. This is for an $8^3 \times 4$ lattice, which is still relatively small, and it indicates that $\mathcal{O}(10^{12})$ more samples would be required in the canonical Monte Carlo approach in order to scan a comparable range of parameter space by ordinary Ferrenberg-Swendsen reweighting techniques.

As another example, in studying first order phase transitions (e.g., [34]), one chooses \mathcal{O}_1 to be the order parameter of the transition; in a model with a scalar field, typically $\mathcal{O}_1 = \int d^4x \phi^2$. One tunes $W[\mathcal{O}_1]$ to cancel the nonperturbative effective potential for this operator, so that the Monte Carlo simulation samples evenly in \mathcal{O}_1 . This enhances statistics for configurations intermediate between the phases. In the mass scan example of Eq. (6.2), one has

$$\langle \mathcal{O} \rangle = \frac{\sum_{C \in F(n)} \mathcal{O}_C \exp(W[\int d^4x \phi_C^2] - \frac{1}{2}(m_2^2 - m_1^2) \int d^4x \phi_C^2)}{\sum_{C \in F(n)} \exp(W[\int d^4x \phi_C^2] - \frac{1}{2}(m_2^2 - m_1^2) \int d^4x \phi_C^2)}. \quad (6.7)$$

In this way, wherever the exponential in (6.7) happens to be at its maximum, a large number of configurations will be generated, due to the flat distribution with respect to $\int d^4x \phi^2$.

Two approaches exist for engineering a good function W .

- (1) One can employ a bootstrap method that iterates between Monte Carlo simulation and adjustments to W . For instance a numerical tabulation of density of states ρ may be obtained from a canonical simulation, as was done in [32, 33]. Schematically, one obtains a histogram estimate of $\rho(\mathcal{O}_1)$ for an operator value range \mathcal{O}_1 range $\mathcal{O}_{1,\min} \leq \mathcal{O}_1 \leq \mathcal{O}_{1,\max}$. This provides an initial version of W , through $W \equiv 1/\rho(\mathcal{O}_1)$. If necessary, the process can be repeated to refine the table.
- (2) Iterative or stochastic searches may be used to optimize W with respect to a predetermined parameterization in a small volume. Performing this at two different small volumes then provides an extrapolation estimate for W in the next largest volume, which can then be refined through another search.

B. Application

If we work at $m_1 \neq 0$, the action that we must tune nonperturbatively is (2.22). If extrapolate to the $m_1 \rightarrow 0$ limit, $U(1)_R$ symmetry (2.13) can be imposed and we must

fine-tune (2.23). We fix y_1 , so that it determines the coupling strength that we study. All other parameters, m_2^2 and λ_1 , are associated with bosonic terms in the action, and can be tuned offline in the way that was just described above.

VII. SIMULATION

A. Pfaffian phase

The integration over lattice fermions yields

$$\text{Pf}(CM), \quad M = \mathcal{D} + mP_+ + m^*P_- + g\tilde{\phi}P_+ + g^*\tilde{\phi}^*P_- \quad (7.1)$$

The transformation

$$\tilde{\chi}(x^0, \mathbf{x}) \rightarrow \gamma^0 \tilde{\chi}(x^0, -\mathbf{x}), \quad \tilde{\phi}(x^0, \mathbf{x}) \rightarrow \tilde{\phi}^*(x^0, -\mathbf{x}), \quad m \leftrightarrow m^*, \quad g \leftrightarrow g^* \quad (7.2)$$

leaves $\tilde{\chi}^T CM \tilde{\chi}$ invariant. Its effect on the Pfaffian is then

$$\text{Pf}(CM)(m, g, \tilde{\phi}) = \text{Pf}(CM)(m^*, g^*, \tilde{\phi}^*) = [\text{Pf}(CM)(m, g, \tilde{\phi})]^* \quad (7.3)$$

so that the Pfaffian is real. There is still the possibility of a sign problem. At weak coupling and $|m|$ not too small this is likely circumvented, since the spectrum of M is pushed away from zero and crossings are avoided. In that case we can work with the phase quenched measure,

$$|\text{Pf}(CM)| = \det(M^\dagger M)^{1/4} \quad (7.4)$$

B. Pseudofermions

The Pfaffian is represented through an integration over bosonic fields, the pseudofermions η , with action

$$S_{PF} = \eta^\dagger (M^\dagger M)^{-1/4} \eta. \quad (7.5)$$

We compute this using the rational approximation

$$(M^\dagger M)^{-1/4} \eta \approx \alpha_0 \eta + \sum_{i=1}^d \frac{\alpha_i}{M^\dagger M + \beta_i} \eta \quad (7.6)$$

where the coefficients α_i, β_i are chosen to minimize errors over the range of eigenvalues of the operator $M^\dagger M$. Since we will work at weak coupling in what follows, we are able to use the spectrum of the $g = 0$ operator, $M_0^\dagger M_0$, to determine this range. In (7.6), the integer d

Lattice	CPU single	GPU (CUDA) single	GPU (Ours) single	CPU double	GPU (CUDA) double	GPU (Ours) double
$8^3 \times 32$	1.1	6.9	24	0.94	4.4	11
$16^3 \times 32$	0.88	14	71	0.69	10	35
$32^3 \times 64$	0.11	20	—	0.085	10	—

TABLE V: Comparison of timing, Gflop/s, for fast fourier transform of the spinor field. Both single and double precision results are given.

is the degree of the approximation. Evaluation of (7.6) requires us to solve the linear algebra problem

$$(M^\dagger M + \beta_i)X_i = \eta \quad (7.7)$$

for each degree $i = 1, \dots, d$. This is done for each i by conjugate gradient, which is an iterative solver designed for sparse linear systems. In computing the $M^\dagger M$ matrix multiplication, we encounter $M f_{in} = f_{out}$ and a similar expression involving M^\dagger . There is a trick for the computation of the “dslash” \not{D} ; we fast Fourier transform the in vector f_{in} to momentum space, apply dslash here where it is diagonal (giving f_{out} in momentum space), then fast Fourier transform back to position space. This avoids an additional layer of rational approximation for computing products involving $(A^\dagger A)^{1/2}$ in position space.

In Table V we give a comparison of timing for fast fourier transform (FFT) of a lattice spinor field such as f_{in} using different tools. Concerning hardware, the CPU runs are from an Intel Xeon Woodcrest 5160, whereas the GPU runs are from a Nvidia GTX 285. The CPU runs were performed using the four-dimensional Numerical Recipes code [36]. The first version of GPU code performs four one-dimensional transforms using the batched CUDA FFT available from Nvidia to get the four-dimensional transform. The second version of GPU code uses our own FFT for the spatial dimensions, which is currently only operational for $L < 32$, due to register constraints. As can be seen, it is quite a bit faster than CUDA FFT. In the temporal dimension $T \geq 32$ so the CUDA FFT is always used in that direction. A necessary reorganizing of the arrays after each of the four one-dimensional transforms is included in the timing. We do not know the origin of the drop in performance of the Numerical Recipes code on large lattices, though it may be related to non-cached memory accesses. We inserted a counter of floating point operations (flop) into the Numerical Recipes code and found that the number of operations was approximately given by $5N \log_2 N$. We used the estimate $5N \log_2 N$ for the number of operations for GPU code as well. What one sees is that even on small lattices the FFT runs an order of magnitude faster using the GPU. Since this is the crucial operation in applying the lattice Dirac operator, we anticipate simulation speeds of approximately 10 Gflop/s for the $16^3 \times 32$ and larger lattices, working in double precision. In what follows we use our own FFT for the $L < 32$ lattices, but the

CUDA FFT for the $L = 32$ lattice.

C. Preconditioning

At weak couplings, we expect that preconditioning by the inverse of the free theory fermion matrix M_0 will improve convergence of the conjugate gradient solver. We must formulate the problem in terms of a hermitian, positive definite matrix. For this purpose, we re-express the problem

$$M^\dagger Mx = b \quad (7.8)$$

as follows:

$$(M_0^{-1\dagger} M^\dagger)(MM_0^{-1})(M_0x) = (M_0^{-1\dagger} b) \quad (7.9)$$

This leads to the definitions

$$\tilde{M} = MM_0^{-1}, \quad \tilde{x} = M_0x, \quad \tilde{b} = M_0^{-1\dagger} b \quad (7.10)$$

The problem in terms of these variables is $\tilde{M}^\dagger \tilde{M} \tilde{x} = \tilde{b}$. Once we obtain \tilde{x} from the conjugate gradient solver, we obtain the desired solution from $x = M_0^{-1} \tilde{x}$, where M_0^{-1} can be computed analytically. It is just

$$M_0^{-1} = \frac{M_0^\dagger}{D_\mu^\dagger D_\mu + |m|^2}, \quad \not{D} \equiv \gamma_\mu D_\mu = (1 - \frac{a}{2} D_2)^{-1} D_1 \quad (7.11)$$

We have solved the problem $M^\dagger Mx = b$ with random Gaussian b on lattices of various sizes, using our GPU code. Convergence is obtained with and without preconditioning. A comparison is given in Table VI. The speed-up factor from the preconditioning is quite large, and the inversion times are rapid enough that simulations on relatively large lattices are realistic.

The pseudofermion η is updated by the heatbath method,

$$\eta = (M^\dagger M)^{1/8} R \quad (7.12)$$

where R is a random complex Gaussian spinor. The $1/8$ power is obtained by rational approximation so that rather than the problem (7.8), we must solve

$$(M^\dagger M + \beta_i)x = b \quad (7.13)$$

for each degree $i = 1, \dots, d$. In order to have high accuracy we have taken $d = 20$. Applying the preconditioning matrix M_0^{-1} then yields

$$\left(\tilde{M}^\dagger \tilde{M} + \beta_i M_0^{-1\dagger} M_0^{-1} \right) \tilde{x} = \tilde{b} \quad (7.14)$$

Lattice	Precision	NPC secs.	NPC iters.	Gflop/s	PC secs.	PC iters.	Gflop/s	speed-up
$8^3 \times 32$	single	1.3	830	14	0.038	8	17	34
$8^3 \times 32$	double	4.9	1600	7.2	0.13	15	8.1	38
$16^3 \times 32$	single	7.1	870	25	0.20	8	31	36
$16^3 \times 32$	double	31	1800	12	0.74	15	13	42
$32^3 \times 64$	single	420	1600	14	6.8	8	15	62
$32^3 \times 64$	double	2200	3900	6.5	25	15	7.0	86

TABLE VI: Timing benchmarks at $m = 1$, $g = 1/5$. PC indicates preconditioning whereas NPC is the inversion without preconditioning. The time in seconds and the number of iterations (iters.) is for convergence. The criterion for convergence is that the relative residual is less than 1×10^{-6} for single precision and less than 1×10^{-12} for double precision. The speed-up is the ratio of NPC time to PC time.

Lattice	Secs.	Gflop/s	Iters.	Secs.	Gflop/s	Iters.
	single	single	single	double	double	double
$8^3 \times 32$	0.93	15	360	3.5	7.5	700
$16^3 \times 32$	4.8	28	370	20	13	730
$32^3 \times 64$	220	14	540	900	6.7	1100

TABLE VII: Pseudofermion heatbath timing benchmarks at $m = 1$, $g = 0.1$, with degree 20 rational approximation of (7.12). Preconditioning is used up to $\beta_i = 100$. The number of iterations is the total over the 20 different degrees.

We find that there is degradation of the speedup due to preconditioning for larger values of β_i . However for very large β_i the problem without preconditioning converges rapidly. Thus we choose a cutoff value, which turns out to be $\beta_i = 100$, above which preconditioning is not used. By this approach we are able to keep the number of iterations for each of the problems (7.13) under 100 for single precision and under 200 for double precision. As Table VII shows, the average number of iterations is far less. For example, at single precision on the $8^3 \times 32$ lattice, a total of 370 conjugate gradient iterations are needed over 20 degrees, for an average of 18.5 iterations for each problem (7.13).

In the molecular dynamics part of the rational hybrid Monte Carlo (RHMC) algorithm, the fermion force terms also require the solution of equations of the form (7.13). These have a performance similar to what is shown in Table VII. We find that approximately 50 steps with double precision are required in order to get good acceptance rates for the Metropolis step that is applied at the end of a molecular dynamics trajectory of length 0.5 simulation time units. We have found that single precision is inadequate for the molecular dynamics evolution. It could however be used for a mixed precision conjugate gradient, as has been promoted in [37].

D. Ward-Takahashi identity

In the continuum the simplest Ward-Takahashi identity is that

$$\langle F \rangle = 0 \tag{7.15}$$

On the lattice this is modified due to the noninvariance of the lattice action. It is therefore of interest to measure $\langle F \rangle$ in our simulations, which as alluded to above use the RHMC algorithm. Working at $ma = 0.5$, $g = 0.1$ we find that sampling over 3283 configurations, after 200 thermalization sweeps,

$$\frac{1}{V} \sum_x \langle F(x) \rangle = [(2 \pm 3) + i(2 \pm 3)] \times 10^{-3} \tag{7.16}$$

The error estimates incorporate an autocorrelation time of approximately 15 sweeps, for this observable. The small value of $\langle F \rangle$ is consistent with the fact that the coupling is weak and at one-loop order in perturbation theory, nonrenormalization of the superpotential is intact. Thus we expect corrections of the scalar potential to start at $\mathcal{O}(|g|^4) = \mathcal{O}(10^{-4})$, roughly consistent with the size of $\langle F \rangle$. Nonsupersymmetric corrections to the scalar potential are required in order to have $\langle F \rangle$ nonzero.

VIII. CONCLUSIONS

We have studied the locality of the Dirac operator that appears in the action (2.17) with fermion matrix (2.19). It was seen in Fig. 1 that there is a long tail on this operator, so that the localization is less pronounced than that of the overlap operator. We found that the scalar self-energy at one-loop takes the form (4.18), so that there is no indication of nonlocality in the external momentum. Thus it may be that the long tail of the operator is harmless.

We established an equivalence between the “untilded” formulation of this lattice theory and the “tilded” theory, at the level of correlation functions in the continuum limit, provided all divergences are logarithmic.

We studied one-loop counterterms in the lattice theory. We have found agreement with previous authors that in the quantum continuum limit of this theory at one-loop, only wavefunction renormalization occurs. We have given numerical values and find that in agreement with what appears in the literature, $Z_\phi = Z_\chi$ but that Z_F is different, in the continuum limit at one-loop.

We described the renormalization of the bare lattice supercurrent. An approach to determining the linear combination that is the symmetry current of the long distance effective theory was outlined. This is crucial for fine-tuning the bare lattice action in the reweighting approach that we are pursuing. We showed that the invariance of the free lattice action does

not have a simple interpretation in terms of a conserved supercurrent, due to the fact that the derivative operators in this formulation are not ultralocal.

We have developed code to run on graphics processing units that are CUDA enabled, and have studied a strategy for handling the inverse square roots of matrices that occur in the theory through fast Fourier transform libraries within CUDA, as well as our own improved version which runs on smaller lattices. We have shown that preconditioning with the inverse of the free theory matrix yields a speed-up that is quite significant in the problems (7.13) that are encountered in an RHMC sweep.

In future work we will fine tune the bare lattice action (2.23) through measurements of identities involving $\partial_\mu S_\mu$, taking an approach that involves reweighting and multicanonical Monte Carlo techniques. We have already measured $\langle F \rangle$ and find it to be quite small at weak coupling. Thus the bare theory without any fine-tuning is a good starting point for the search over parameter space. An incremental search strategy, starting at weak coupling, moving gradually to stronger coupling, looks realistic.

Acknowledgements

This research was supported in part by the Dept. of Energy, Office of Science, Office of High Energy Physics, Grant No. DE-FG02-08ER41575 as well as Rensselaer faculty development funds. We are grateful to members of the Boston University QUDA development group (Ron Babbich, Richard Brower and Mike Clark) for providing us a copy of their GPU code, which we borrowed from and used as a template for our own GPU code. We thank Georg Bergner and Alessandro Feo for helpful discussions and communications.

-
- [1] K. Fujikawa and M. Ishibashi, Nucl. Phys. B **622** (2002) 115 [arXiv:hep-th/0109156].
 - [2] K. Fujikawa and M. Ishibashi, Phys. Lett. B **528** (2002) 295 [arXiv:hep-lat/0112050].
 - [3] K. Fujikawa, Nucl. Phys. B **636** (2002) 80 [arXiv:hep-th/0205095].
 - [4] M. Bonini and A. Feo, JHEP **0409** (2004) 011 [arXiv:hep-lat/0402034].
 - [5] Y. Kikukawa and H. Suzuki, JHEP **0502** (2005) 012 [arXiv:hep-lat/0412042].
 - [6] M. Bonini and A. Feo, Phys. Rev. D **71** (2005) 114512 [arXiv:hep-lat/0504010].
 - [7] J. Giedt, PoS **LAT2006**, 008 (2006) [arXiv:hep-lat/0701006].
 - [8] J. Giedt, Int. J. Mod. Phys. A **21**, 3039 (2006) [arXiv:hep-lat/0602007].
 - [9] J. Giedt, Int. J. Mod. Phys. A **24** (2009) 4045 [arXiv:0903.2443 [hep-lat]].
 - [10] S. Catterall, D. B. Kaplan and M. Unsal, Phys. Rept. **484** (2009) 71 [arXiv:0903.4881 [hep-lat]].
 - [11] A. Feo, Mod. Phys. Lett. A **19** (2004) 2387 [arXiv:hep-lat/0410012].
 - [12] I. Montvay, Int. J. Mod. Phys. A **17**, 2377 (2002) [arXiv:hep-lat/0112007].

- [13] G. T. Fleming, J. B. Kogut and P. M. Vranas, *Phys. Rev. D* **64**, 034510 (2001) [arXiv:hep-lat/0008009].
- [14] J. Giedt, R. Brower, S. Catterall, G. T. Fleming and P. Vranas, in proceedings Workshop on Continuous Advances in QCD 2008, Minneapolis, Minnesota, 15-18 May 2008, ed. M. Peloso, World Scientific, Singapore, 2008, arXiv:0807.2032 [hep-lat].
- [15] M. G. Endres, in proceedings 26th International Symposium on Lattice Field Theory (Lattice 2008), Williamsburg, Virginia, 14-20 Jul 2008, arXiv:0810.0431 [hep-lat].
- [16] J. Giedt, R. Brower, S. Catterall, G. T. Fleming and P. Vranas, *Phys. Rev. D* **79**, 025015 (2009) [arXiv:0810.5746 [hep-lat]].
- [17] M. G. Endres, *Phys. Rev. D* **79** (2009) 094503 [arXiv:0902.4267 [hep-lat]].
- [18] M. G. Endres, arXiv:0912.0207 [hep-lat].
- [19] J. W. Elliott, J. Giedt and G. D. Moore, *Phys. Rev. D* **78**, 081701 (2008) [arXiv:0806.0013 [hep-lat]].
- [20] B. A. Berg and T. Neuhaus, *Phys. Lett. B* **267** (1991) 249.
- [21] M. Falcioni, E. Marinari, M. L. Paciello, G. Parisi and B. Taglienti, *Phys. Lett. B* **108** (1982) 331.
- [22] A. M. Ferrenberg and R. H. Swendsen, *Phys. Rev. Lett.* **61** (1988) 2635.
- [23] A. M. Ferrenberg and R. H. Swendsen, *Phys. Rev. Lett.* **63** (1989) 1195.
- [24] H. Neuberger, “Exactly massless quarks on the lattice,” *Phys. Lett. B* **417** (1998) 141 [arXiv:hep-lat/9707022].
- [25] M. Luscher, *Phys. Lett. B* **428** (1998) 342 [arXiv:hep-lat/9802011].
- [26] L. H. Karsten and J. Smit, *Phys. Lett. B* **85**, 100 (1979).
- [27] P. Hernandez, K. Jansen and M. Luscher, *Nucl. Phys. B* **552** (1999) 363 [arXiv:hep-lat/9808010].
- [28] H. B. Nielsen and M. Ninomiya, *Phys. Lett. B* **105** (1981) 219.
- [29] H. B. Nielsen and M. Ninomiya, *Nucl. Phys. B* **185** (1981) 20 [Erratum-ibid. *B* **195** (1982) 541].
- [30] K. Binder, *Z. Phys.* **B43** (1981) 119.
- [31] B. Baumann, *Nucl. Phys. B* **285** (1987) 391.
- [32] P. de Forcrand and O. Jahn, *Nucl. Phys. B* **651** (2003) 125 [arXiv:hep-lat/0211004].
- [33] P. de Forcrand and O. Jahn, Proceedings of the NATO workshop on “Confinement, Topology, and other Non-Perturbative Aspects of QCD”, Stara Lesna, Feb. 2002,” hep-lat/0205026,
- [34] K. Kajantie, M. Laine, K. Rummukainen and M. E. Shaposhnikov, *Nucl. Phys. B* **466** (1996) 189 [arXiv:hep-lat/9510020].
- [35] G. D. Moore and K. Rummukainen, *Phys. Rev. D* **63** (2001) 045002 [arXiv:hep-ph/0009132].
- [36] W. H. Press, S. A. Teukolsky, W. T. Vetterling and B. P. Flannery, “Numerical Recipes in C: The Art of Scientific Computing,” 2nd ed., Cambridge University Press, New York, 1992.
- [37] M. A. Clark, R. Babich, K. Barros, R. C. Brower and C. Rebbi, arXiv:0911.3191 [hep-lat].